# A LOW-NOISE, LOW-POWER CMOS AMPEROMETRIC CIRCUIT FOR GLUCOSE SENSING

by

NIRANJAN KARANDIKAR

Presented to the Faculty of the Graduate School of

The University of Texas at Arlington in Partial Fulfillment

of the Requirements

for the Degree of

DOCTOR OF PHILOSOPHY

THE UNIVERSITY OF TEXAS AT ARLINGTON

DECEMBER 2013

Acknowledgements

Firstly I would like to thank my PhD advisor Dr. Sungyong Jung for giving me this opportunity. I have learnt a lot of valuable things from him. When I joined his lab in Spring 2007 I had no idea of how to conduct research, he taught me various aspects of research by being extremely patient and motivated me from time to time. I will be indebted to him for the rest of my life.

I will also like to thank my committee members Dr.Wetz, Dr.Schizas, Dr.Dillon and Dr.Choi. I would also like to Dr. Davoudi for lending us equipments which helped me for my research. I want to mention the electrical engineering department assistants, Gail, Ann, and Janice for their constant and kind assistances.

I take this opportunity to thank all current and previous members of my lab, AMIC- Dr. Varun Shenoy, Dr.J.C.Lee, Dr. Partha Ghosh, Mr. Tim Merkin, Mr. Sunil Govardhan, Mr. Sujith Dermal. I had a wonderful time working with you all and I will always cherish it.

During these years at UTA I have met many wonderful friends without their help and support this work would have been impossible, I would like to thanks all of them. I would also like thank my dear friends Prashant, Kalpita and Rizwan who were always there to help me.

Finally I would like to thank my parents and my sister for their continuing support. My wife, who is also doing her PhD, is my constant source of support and motivation. Being a fellow PhD student she understands the ups and downs in a life of PhD student. Without her constant motivation this work would have been impossible. I would like to thank her for all the love and support.

.

October 16, 2013

Abstract

A LOW-NOISE, LOW-POWER CMOS AMPEROMETRIC

CIRCUIT FOR GLUCOSE SENSING

Niranjan Karandikar, PhD

The University of Texas at Arlington, 2013

Supervising Professor: Sungyong Jung

Diabetes is a disorder associated with an insufficiency of insulin secretion. Large number of people around the world suffers from this disorder which can result in damages to eyes, kidneys, nerves and even death. One of the most common methods to detect the diabetes is to monitor the levels of glucose in the blood stream. Other biological fluids like tear fluid can also be used to detect levels of glucose. With emergence of MEMS technology several biosensors have been developed, less invasive or non-invasive, which can detect these glucose levels from blood or tears. The Central idea behind the developments of these biosensors is to have a glucose monitoring system which is portable and/or implantable.

In this work, two novel circuit architectures for glucose sensing are presented. First architecture can be used to detect glucose levels from blood while the second architecture, called wide dynamic range architecture, can be used to detect glucose levels from blood samples and from tear fluid. Existing circuit architectures requires two separate circuits one to control reaction potential, often called potentiostat, while other to readout reaction current. All of the architectures are based on operational amplifiers and do not fully appreciate the power of integrated circuits. These architectures are power

hungry and noisy. Architectures presented in this work are less power hungry, generate less noise and are compact.

Architecture proposed for glucose sensing from blood occupies 125µm*340µm of area while consuming 199µW of power and generating 312µVrms noise. Circuit is shown to measure glucose levels from 2.5mM to 10mM. Wide dynamic range architecture can be used to detect glucose levels either from blood or from tear fluid. Circuit occupies 116µm*551µm area while consuming 217.6µW of power and generating 444µVrms noise. Circuit is shown to detect glucose levels from 1mM to 10mM.

Table of Contents

List of Illustrations

List of Tables

# Chapter 1

## Introduction

Before we began understanding how we can build optimum circuit architecture for glucose sensing it is instructive to evaluate why we need to measure the glucose levels. When we intake the food it is digested by stomach. Carbohydrates from the food are then converted to another form of sugar called glucose. This glucose is then released in blood and carried out to different cells and organ. Cells need insulin to use glucose for energy. Insulin is a hormone secreted by pancreas. If body fails to generate enough insulin or cannot not respond to the insulin the glucose levels in the blood rises giving rise to a disorder called Diabetes [1].

Glucose levels in the blood are classified in three categories namely Euglycemia, Hypoglycemia and Hyperglycemia. Euglycemia is a condition when blood sugar levels are between 4mM-7mM and is considered to be normal. In Hypoglycemia blood sugar levels are less than 4mM and can lead to fainting, comma and even death. Hyperglycemia is characterized by blood sugar levels higher than 7mM and can lead to damages to eyes, kidneys, nerves etc [2]. Even though sensing glucose levels from blood is most popular method, several other methods like sensing glucose concentration from tear fluid are also available. Tear fluid is directly accessible from the eye and can be used as a chemical interface between the sensor and the human body. Different levels of glucose concentrations are reported in tear fluid, depending on the amount of tear analyzed, and they range from few hundreds of µM to few mM [3][4][5].

There are two types of Diabetes; in type 1 diabetes, body does not produce enough Insulin while in type 2 diabetes body fails to respond to the insulin produced. Approximately 285 million adults (age between 20 and 79) suffer from Type-1 and/or Type-2 diabetes and this number is expected to increase to 430 million adults by 2030 [6]

Constant monitoring glucose levels are very important for diabetic people. Several commercially available glucose meters are available for this purpose. Glucose meter has

two parts; one is the referred to as a test strip and another as a interfacing circuit. Test-strip is a small electrochemical cell which converts glucose concentration into proportional current. Figure 1-1 shows the interfacing circuit used for glucose meters.

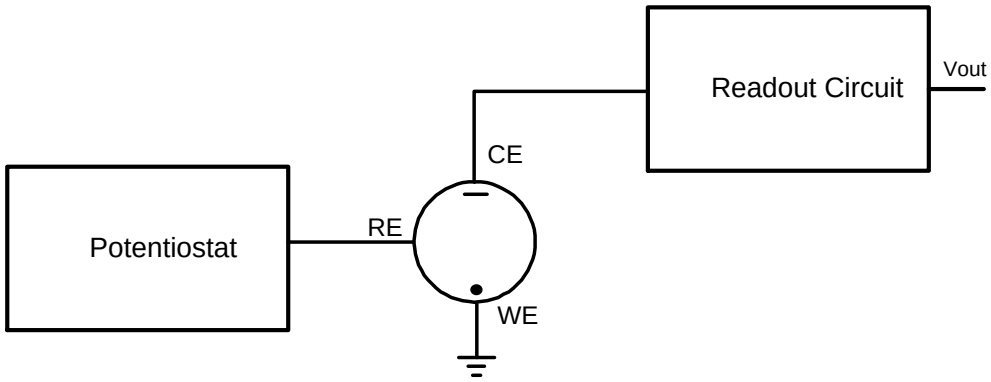


Figure 1-1 Electronic Interfacing circuit for glucose meter

Interfacing circuit has two components- a potentiostat maintains a constant potential between reference and a working electrode which is required for reaction. Reaction current is then read by current readout circuit which converts reaction current into voltage.

Handheld glucose meters are only one of the methods to monitor the glucose levels. Now a days there is a lot of research to use smart-phone as a glucose meter. Implantable glucose sensors which can monitor glucose levels in real time are also a subject of great research. These new applications require new circuit architectures to

meet the specifications forced by them. Figure 1-2 shows the architecture requirements for glucose sensing circuits designed for these future applications.

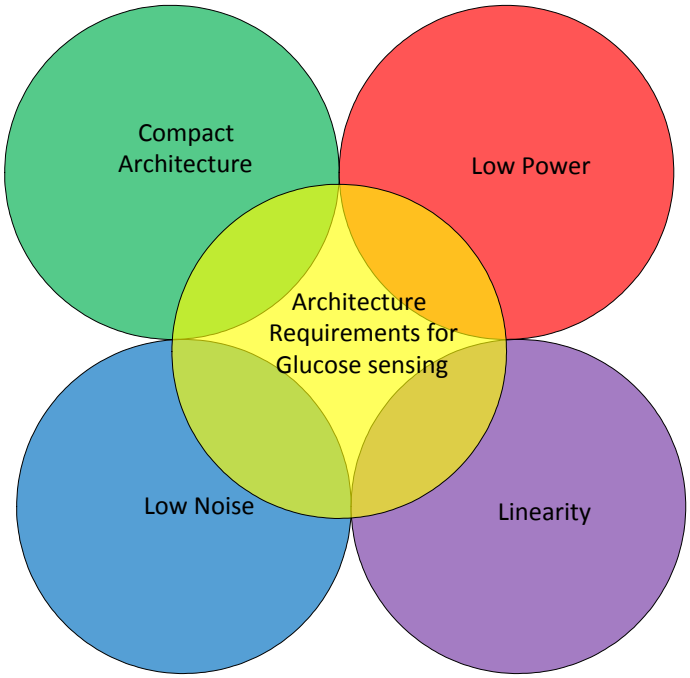


Figure 1-2 Architecture Requirements for glucose sensing

Since these applications, either smart phone integration or implantable glucose sensors are ultra-mobile one of the most important architecture requirement is power dissipation. Lower the power consumed by interfacing circuit larger the battery life. Another important factor is compactness or area requirements. Small form factor or compactness is very important for designing interfacing circuit for these applications. Low noise and high linearity ensures a good quality readout circuits and they are very crucial.

One of the most widely used circuit architecture for glucose sensing is trans-impedance amplifier [7]. This configuration is simple and effective for discrete implementation of readout circuit but suffers many disadvantages in integrated approach for portable applications such as large area, power and noise. Another disadvantage of

this circuit is larger feedback resistor, used to convert current into voltage, required for sensing smaller currents. This requires larger area and generates higher noise [8]. Architecture described in [9] uses instrumentation amplifier to sense the voltage that is developed across resistor $R_{M.}$ This approach uses large number of transistors and hence generates larger noise and consumes more power. Noise reduction is achieved in architecture described in [10] using switched capacitor circuit to read current. Switched capacitor circuit needs multiple switches and good phase locking between various switches. This makes architecture complex and consumes large power thus making it unsuitable for portable applications. Circuit shown in [11] uses a resistor inserted between working electrode and ground while voltage developed across it is sensed. This approach causes the potential of working electrode to change depending upon the current thus making proper potential control at working electrode difficult [8]. Current mirror circuit used to sense/amplify the sensor current is presented in [8]. This architecture still uses operational amplifier for potential control as a results is not compact. It can thus be seen from all the above mentioned architectures, that reference voltage is maintained by a separate opamp while method to sense the resulting current varies. As a result it can be seen that existing circuit architectures do not satisfy all these requirements.

The objective of this work is to design a low power, low noise, compact architecture for future applications like smartphone glucose sensor and implantable glucose sensor etc. In this work two novel architectures for glucose sensing are proposed. First architecture is can be used for glucose sensing from blood samples and it is shown that architecture can detect glucose levels from 2.5mM-10mM there by covering all three conditions of Euglycemia, Hypoglycemia and Hyperglycemia. Second architecture is wide range, variable gain architecture which can be used to detect glucose

levels from blood samples as well as from tear fluid. Architecture is shown to detect glucose levels from 1mM-10mM. Both the architectures are low power, consuming around 199μW of power, low noise, generating around 450μVrms noise. These architectures are thus suitable for the future applications.

This dissertation is organized as follows

Chapter 1 introduces to the need for sensing/monitoring glucose levels; it also lists the ill effects of diabetes. Current methods to monitor glucose levels are described in brief at same tine future trends in monitoring glucose levels are mentioned. It also covers the research objective and motivations.

Chapter 2 covers the background of electrochemistry and glucose sensors. It also surveys in detail current circuit architectures used for glucose sensing with advantages and drawbacks.

Chapter 3 presents the proposed architecture for glucose sensing from blood samples. This chapter presents all the theory with required analysis showing advantages of the present architecture over others. Simulation results and measurement results are presented to validate the circuit performance.

Chapter 4 discusses variable gain architecture which can be used to detect glucose levels from blood samples and tear fluid. Simulation and measurements results are included to validate the working.

Chapter 5 concludes the dissertation by summarizing the work and detailing the advantages of the work.

# Chapter 2

## Background

### Basics of electrochemistry

Commercially available glucose sensors are generally electrochemical sensors thus it is instructive to understand the basics of electrochemistry. Electrochemistry is the branch of chemistry which explores the relation between chemistry and electricity. Some chemical reactions that proceed spontaneously can generate electrical current, which can be used to do useful work; while other chemical reaction can be forced to proceed by using electrical current. Many practical devices are based on these reactions, and many products made by these reactions are well-known, everyday household items [12]. We can find several examples around us where electrochemistry is used. Normal batteries, for example, use electrochemistry. The batteries contain certain chemicals in them these chemicals reacts under certain conditions to produce electrical current. This current can then be used to carry out different operations. All the electrochemical reactions are invariably oxidation and reduction reactions. When chemical reaction occurs some atoms/molecules donate electrons while others receive electrons. Atoms/molecules which donate electrons are said to be oxidized while the ones who receive electrons are said to be reduced [12][13].

Let's understand how electrochemical reactions occur by a simple example of silver electrode immersed in pure water (Figure 2-1)[13]. When silver electrode is immersed in the water, silver atoms are dissolved in the water, as positive ions, leaving electrons behind on the silver electrode; reaction is expressed by following equation (1)

$$Ag \rightarrow Ag^{+} + e^{-} \tag{2.1}$$

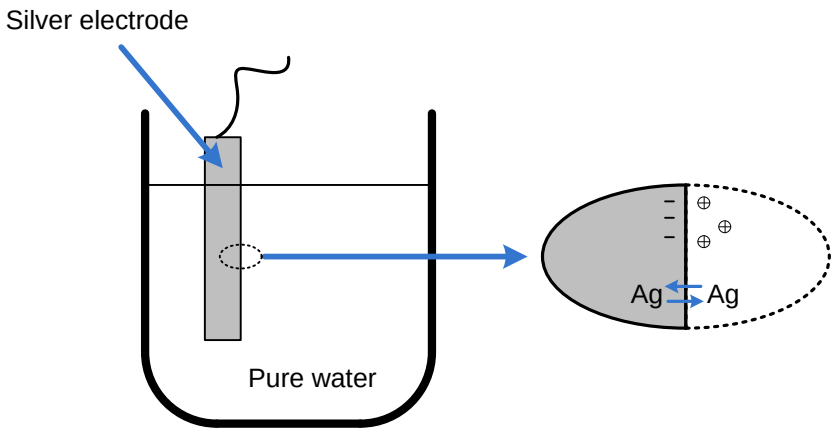


Figure 2-1 Oxidation of silver electrode immersed in water [13]

As more and more ions dissolve in water potential gradient is developed between electrode and water. This potential difference is referred to as interfacial potential difference, which can affect the rate and direction of the reaction. Different electrodes have different interfacial potential differences. As briefly explained before, the two basic types of charge transfer reactions take place at an electrode solution interface: oxidation and reduction. During an oxidation reaction, the chemical species transfer electron(s) to the electrode, while in a reduction reaction; the chemical species receive electron(s) from the electrode. The resulting chemical reactions are represented as:

Oxidation

$$R \rightarrow O + ne^{-} \tag{2.2}$$

Reduction

$$O + ne^{-} \rightarrow R \tag{2.3}$$

where O is the oxidized species, R is the reduced form of species and n is the number of electrons transferred during the reaction.

A very large potential gradient exists on the electrode/electrolyte interface. The interfacial potential difference, E, of an electrode can be calculated using the Nernst equation [13]

$$E = E^0 + \frac{RT}{nF} ln\left(\frac{C_o}{C_R}\right) \quad (2.4)$$

$E^0$ is the standard potential of the electrode, R is the molar gas constant, T is temperature, F is Faraday's constant and $C_o$ and $C_R$ are the concentration of the oxidized and reduced forms of the species, respectively. In order to make use of electrochemistry it is important that oxidation and reduction sites are physically separated. The electrons, rather than just hopping from one atom or molecule to the other, are forced to move through an external wire, and the resulting electrical current [12]

## Electrochemical Sensors

Electrochemical sensors are used for variety of applications ranging from detection of toxic gases to understanding blood glucose levels [14]. The idea behind electrochemical sensors is to produce electrical signal (potential, current or impedance) which is proportional to chemical reactions there by quantifying different aspects of reactions, for example concentration and presence of certain chemicals. Electrochemical sensors are thus classified into three categories [14] [15] namely Potentiometric sensors, Conductometric sensors and Voltammetric sensors

*Potentiometric sensors*

Open circuit potential of electrochemical cell is measured in Potentiometric sensors. Due to chemical reactions this open circuit potential changes as shown by Nernst's equation. According to Nernst's equation the change in potential is proportional to the logarithm of the concentration of the chemical species of interest. Since potential change has a logarithmic response, potentiometric sensors are useful when concentration of chemical species changes on the few order of magnitude like measurement of pH [16]. Glucose concentration changes only on the order magnitude thus potentiometric sensors are not very useful. On the other hand, a sensor with a linear relationship between response and concentration is preferable (such as Amperometric sensors) rather than logarithmic response [7].

*Conductometric sensors*

In conductometric sensors conductance (which is reciprocal of resistance) of a material changes when it interacts with certain chemical species [16]. Conductance is measured by an alternating current bridge method. Since it is conductance (not impedance), measurement is performed at one fixed frequency [17].

*Voltammetric Sensors*

In voltammetric sensors, the voltage is applied across the electrodes of the electro-chemical cell and the current flowing between them is measured. The measured current is due to the response of chemical species of interest. Different types/shapes of input signals like linear, square or triangular can be applied in Voltammetry. If a periodic triangular voltage waveform is applied between the working and the reference electrodes and the current response of the cell is monitored then the technique is called as cyclic

voltammetry. Cyclic voltammetry is commonly used for microelectrode (i.e., electrodes with dimensions on the order of micrometers) to reduce the non-faradaic current. In chronoamperometry electrochemical analytical technique, the potential of the working electrode is stepped, and the resulting faradaic current (caused by the stepped potential) is measured as a function of time [13]

*Amperometric Sensors*

In voltammetric sensors if the voltage is kept constant and the resulting reaction current is measured then the technique is called as Amperometry. Thus amperometric sensors are special type of voltammetric sensors. Role of Ohms law is very evident is amperometric sensors [16]. The measured current is a function of the concentration of the electroactive species. The response will have high linearity if the current is limited by the rate of the mass transfer and not by the rate of charge transfer [13] .

Classification of amperometric Glucose biosensor

Amperometric Glucose biosensors are generally classified as $1^{st}$, $2^{nd}$ and $3^{rd}$ generation of biosensor. Before we understand the three generations of glucose biosensors, it is important to understand the meaning of biosensors. Biosensors are generally sensors which uses biological agents like enzymes to detect chemical reactions or to detect certain chemicals [18]. Fast response, accuracy, sensitivity, range and stability are important specifications of the glucose biosensors[7]. The Equation (2.5) shows the typical reaction that takes place in glucose detection. The reaction can be better explained with the help of Figure 2-2. In a typical glucose sensor, working electrode is coated with an enzyme (which is nothing but catalyst) called glucose oxidase which has affinity towards glucose. In normal conditions, glucose oxidase enzyme oxidizes with the glucose to form gluconic acid, changes into an inactivated reduced state

by accepting electrons. This reduced enzyme returns to active oxidized state by giving these electrons to molecular oxygen and thereby producing hydrogen peroxide (H2O2) [19] [20].

$$Glucose + O_2 \xrightarrow{GOx} Gluconice\ Acid + H_2O_2 \quad (2.5)$$

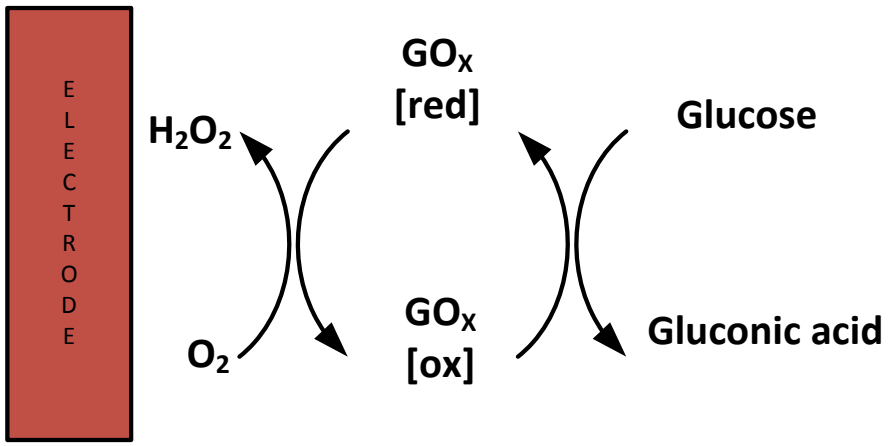


Figure 2-2 Enzymatic reaction between glucose and glucose oxidase [20]

All three types of electrochemical sensors can be used to detect the glucose concentration[7].Potentiometric sensors which detect changes in potential can be used since solution pH levels change because of the formation of gluconic acid. Conductometric sensors can be used as reaction changes the solution resistance. Amperometric (which are type of voltametric sensors) sensors can be used by measuring the amount of oxygen consumed or by measuring the amount of hydrogen peroxide produced in the reaction. Amperometric glucose biosensors are the most widely used glucose biosensors as they produce linear response to glucose concentration.

*First Generation of Electrochemical Glucose Biosensors*

First generation of glucose biosensors use oxygen substrate and measure the amount of hydrogen peroxide produced. Measurement of hydrogen peroxide is very simple and generally carried out using platinum electrode which is 0.6V higher than silver/silver chloride electrode. First generation glucose bio sensors suffer from errors like change in sensors response and linearity due to oxygen dependence [21].

*Second Generation of Electrochemical Glucose Biosensors*

Second generation glucose biosensors use mediators to transfer electrons from glucose oxidase to the electrode. Mediator thus eliminates the limiting factor of transferring electrons from glucose oxidase to the electrode [21]. The drawbacks associated with these sensors is that, mediator could leak out of the electrode surface, and secondly most of the proposed mediators are toxic, which makes their implantation hazardous [7]

*Third Generation of Electrochemical Glucose Biosensors*

Eliminating the mediator and achieving low operating potential are the most important characteristics of third generation glucose biosensors. This gives high selectivity to the biosensors [21] [22].

## Enzymatic and Non-enzymatic glucose sensors

*Enzymatic glucose sensors*

Enzymatic glucose biosensors use enzyme, like glucose oxidase which has higher affinity towards glucose, for detection of glucose. These sensors are most popular and dominate the market of glucose biosensors. As discussed above enzymatic glucose

biosensors (1st,2nd and 3rd generation) have many issues like oxygen dependence , mediator leak , larger operating potential etc.. Common drawbacks of enzymatic glucose sensors are insufficient sensor data stability, complexity of the enzyme immobilization, and oxygen [23] . As a result there is a lot of research in eliminating the need of using enzyme for glucose detection [24] [25].

*Non-Enzymatic glucose sensor*

Non-enzymatic glucose biosensors do not use enzyme for glucose detection. As a result they are sometimes referred to as fourth generation of glucose biosensors. Non-enzymatic glucose sensors directly oxidise the glucose in the sample [24]. Direct glucose oxidation at a noble metal electrode which has a large surface area shows considerable signal to noise ratio allowing for the measurement of glucose in blood without the use of an enzyme [24]. One of the main issues of the non-enzymatic glucose sensor design is the low sensitivity.. With advancements in nanotechnology, the sensitivity of non-enzymatic glucose sensors based on direct oxidation on the nanoporous electrode has risen considerably and gives physiologically useful sensitivity[24]. Nano-scale electrodes make a very high electro-active surface area that is considerably larger than the geometric surface area, resulting in enhancement of electro-catalysis [26] [19].

Two and three terminal glucose sensors

Typically there are two types of electrochemical cells, two terminals and three terminals. Two terminal electrochemical cells have two electrodes called as working electrode and reference electrode, as shown in Figure 2-3. Working electrode is the electrode where the reaction of interest takes place. Reference electrode provides a potential at working electrode so that reaction can occur. It also provides the path for

reaction current. As the reaction current flows from the reference electrode it becomes polarized. The potential difference between working electrode and reference electrode is also not kept constant. This issue is resolved in tree terminal electrochemical cell.

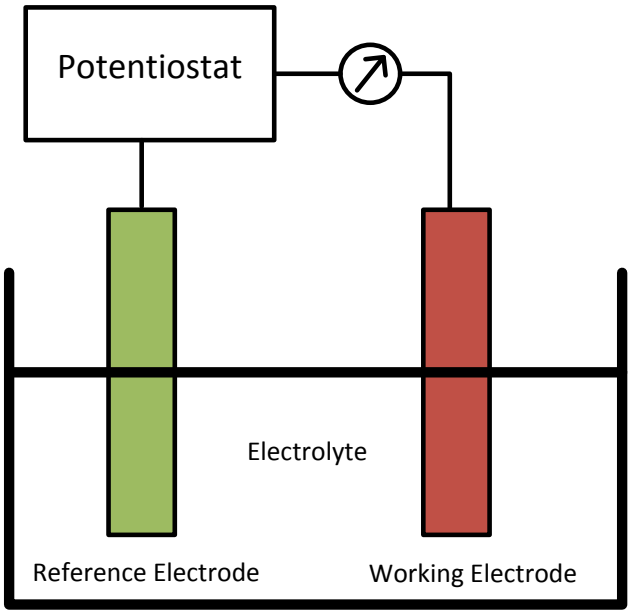


Figure 2-3 Two terminal electrochemical sensors

Three terminal electrochemical cell is shown in Figure 2-4. It has an additional electrode which is referred to as auxiliary electrode. Like two terminal cell, working electrode is where reaction of interest takes place and they are coated with certain enzyme to increase the sensitivity to a specific species for example in the case of glucose case it is glucose oxidase. Reference electrode provides the stable potential to working electrode for the reaction to occur, while counter electrode shunts the current away from reference electrode. As a result no current flows from the reference electrode. Thus three electrode sensors control potential accurately than two electrode sensors. Architectures developed in this work can be used for both the types of electrochemical

cells. Three terminal electrochemical cells are widely used in glucose sensing owing to reasons mentioned before.

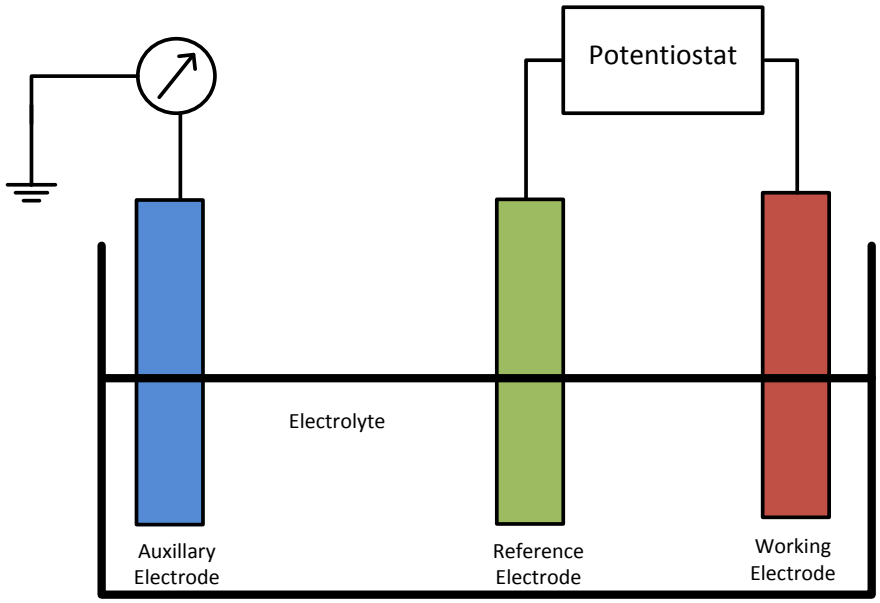


Figure 2-4 Three terminal electrochemical cell

*Electrical Model of electrochemical sensor*

Electrochemical cell is where chemical reactions take place. Glucose sensors are nothing but small electrochemical cells. In order to design a proper electronic interface circuit for electrochemical cells it is important to have electrical equivalent circuit for electrochemical cell. Figure 2-5 shows electrical equivalent circuit for three terminal electrochemical cell. $C_{ce}$ and $C_{we}$ is the double layer capacitances of CE and WE. RCE, RRE and RWE represent the charge transfer resistances of the CE, RE, and WE. Rs1 and Rs2 represent the solution resistance [17]. Table 2-1 lists different components in the electrical model for the sensor. The impedance of an electrochemical cell is usually experimentally measured over a wide frequency range (usually from 1 mHz to 20 kHz) and then, using a non-linear least squares fitting program, an equivalent circuit is fitted to

the experimental data. In Electrochemical Impedance Spectroscopy (EIS), the impedance of an electrochemical cell is measured over a frequency range. This is a powerful tool for the analysis of complex electrochemical systems and to experimentally model the electrical equivalent circuit of the electrochemical cell (working, reference, counter electrodes and solution resistances) [27].

Table 2-1 Sensor model component description

| **Component** | **Description** |
|---|---|
| Cce,Cwe | Double layer capacitances |
| Rce,Rre,Rwe | Charge transfer resistances |
| Rs1,Rs2 | Solution resistances |

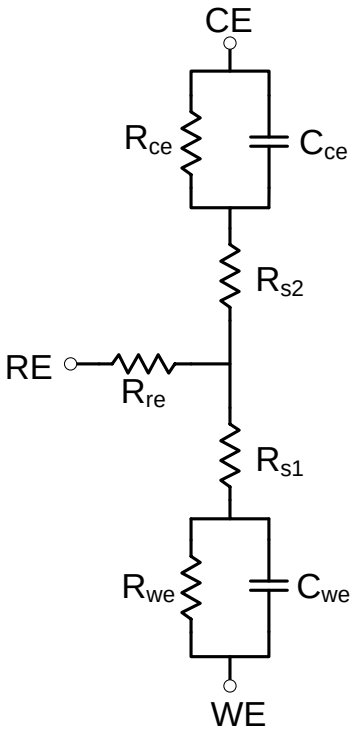


Figure 2-5 Electrical equivalent model electrochemical sensor

Electronics Interfacing circuits glucose sensors

As sensors used for sensing glucose from blood and tear fluid use the same electrochemical principle similar electronic interfacing circuits are used. Figure 2-6 shows the architecture of electronic interfacing circuit with glucose sensor. Circuit consists of two parts, potentiostat and current readout circuit. Potentiostat is a circuit which maintains constant potential between working electrode and counter electrode. While current readout circuit converts the reaction current, proportional to glucose concentration, into voltage. Different architectures discussed here use the same principle

of the two circuit approach. Most common architecture used is called trans-impedance amplifier architecture as shown in Figure 2-7.

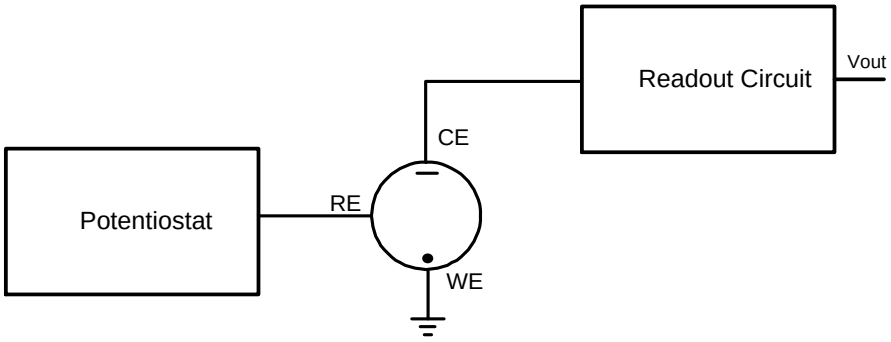


Figure 2-6 Architecture of electronic circuit used with glucose sensor

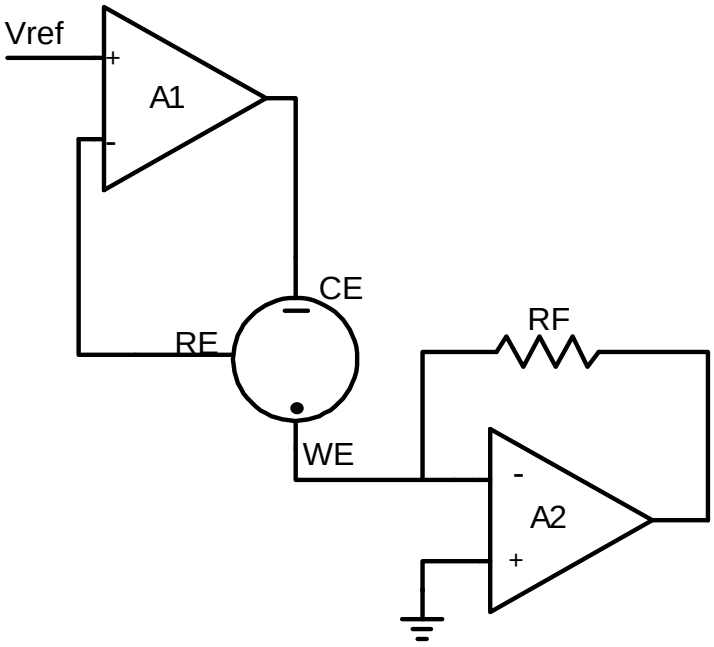


Figure 2-7 Trans-impedance amplifier architecture

Amplifier A1 acts as potentiostat which maintains constant voltage Vref at RE and supplies current through CE while amplifier A2 acts as a trans-impedance amplifier and converts current coming from WE to output voltage. Working electrode (WE) is maintained at ground potential as it is connected to virtual ground. This configuration is effective for discrete implementation of readout circuit but suffers many disadvantages in integrated approach for portable applications such as large area, power and noise. Trans-impedance amplifier uses resistive feedback to convert current into voltage. Another disadvantage of this circuit is that larger feedback resistor is required for sensing smaller currents. This requires larger area and generates higher noise. It should also be noted that working electrode is not connected to actual ground but to virtual ground and thus can pick up environmental noise [28]. Another architecture is presented in [29] and shown in Figure 2-8.

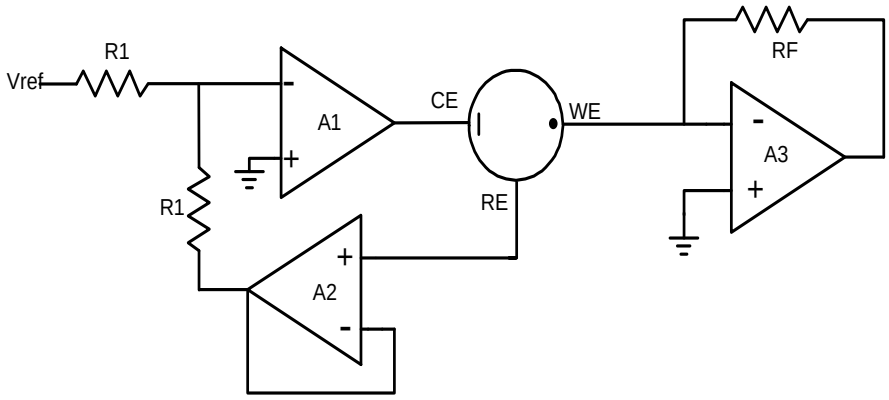


Figure 2-8 Trans-impedance amplifier variant architecture [29]

This architecture is similar to the one described before with an exception of an amplifier A2. Amplifier A2 acts as buffer amplifier and it buffers the Vref to the reference electrode.

In the process it also presents very high input impedance to reference electrode and thus avoiding current flow out of reference electrode. Thus, the architecture provides a better and accurate potential control but carries all the disadvantages of previous architecture. Because of amplifier A2, this architecture is more complex, consumes more power and generates more noise. Switched capacitor architecture [10] is a low noise architecture and is shown in Figure 2-9. Architecture still uses OPAMP based potentiostat architecture but uses switched capacitor Trans- impedance amplifier. OPAMP A3 and capacitor C1 acts as an integrator there by integrating sensor current and converting it to voltage.

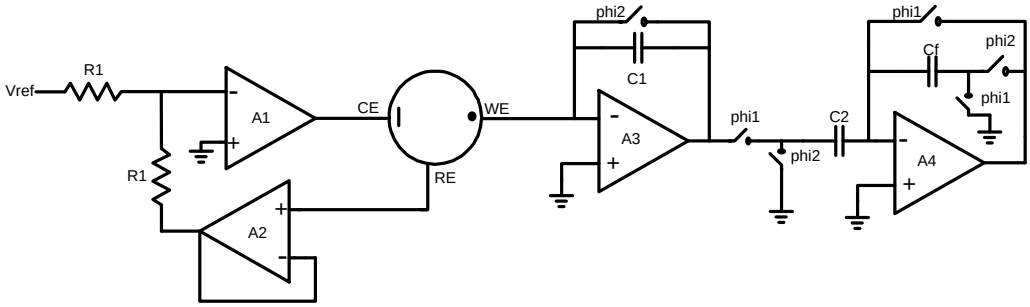


Figure 2-9 Switched capacitor architecture [10]

OPAMP A4 along with capacitors C2 and Cf acts as voltage amplifier whose gain is nothing but the ratio of two capacitors. Architecture generates lower noise because of technique called as correlative double sampling (CDS). Switched capacitor architecture is more complex than the previous architectures and thus consumes more power. Also one has to generate two non-overlapping clocks phi1 and phi2 which adds to both complexity and power. There are several types of architectures used for sensing current generated by working electrode. Architecture described in [9] and shown in Figure 2-10 uses instrumentation amplifier to sense the voltage that is developed across resistor RM.

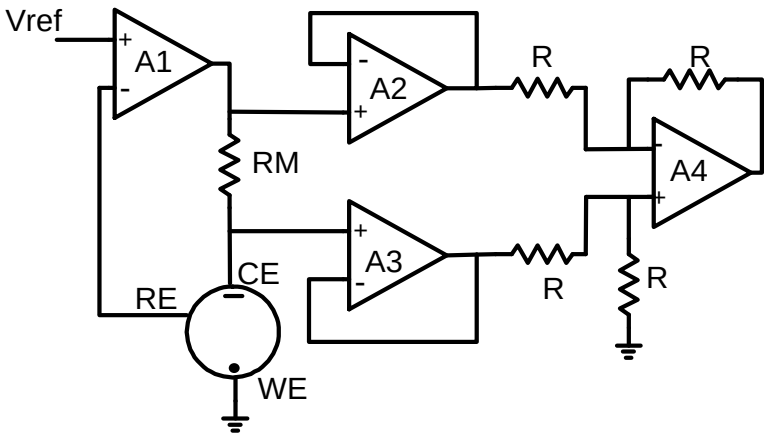


Figure 2-10 Instrumentation amplifier architecture [9]

This approach uses large number of transistors and hence generates larger noise and consumes more power. One of the advantages of this architecture is that working electrode is connected to actual ground instead of virtual ground and thus does not pick environmental noise. In another approach as shown in Figure 2-11 resistor is inserted in between working electrode and ground and voltage developed across it is sensed [11]. This approach changes the potential of working electrode depending upon the current and thus proper potential control at working electrode is difficult [8].

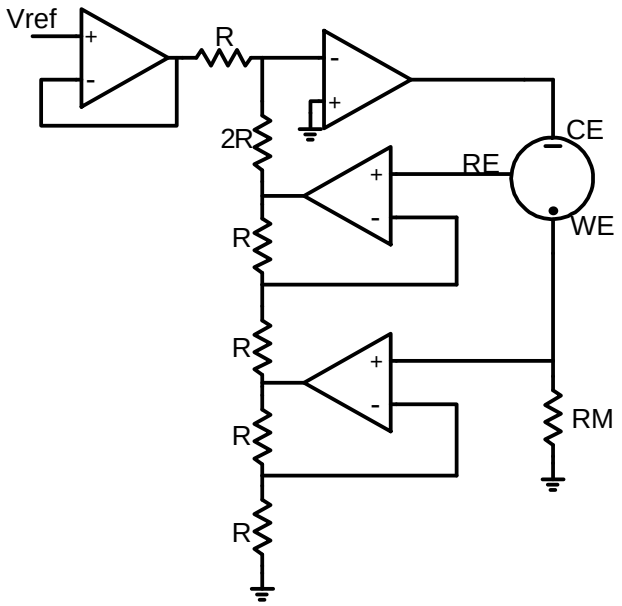


Figure 2-11 Modified current readout architecture [8]

More compact approach is presented in [8], shown in Figure 2-12, which uses current mirror circuit to sense/amplify the current. Architecture still needs OPAMP to control the potential. Also reference voltage needs to generate either internally or externally.

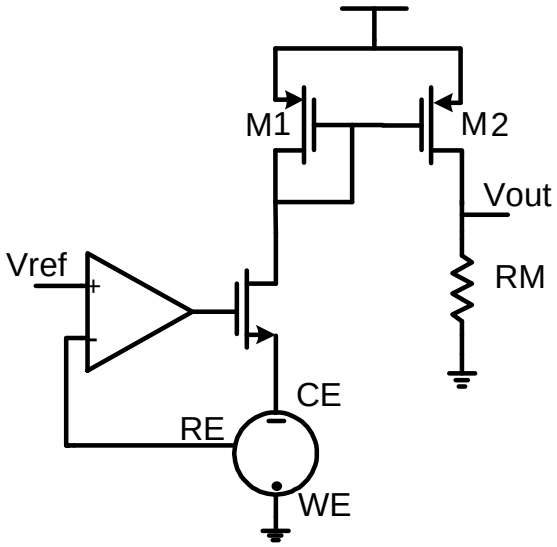


Figure 2-12 Current Mirror based architecture [8]

Summary of different architectures is presented below.

- Two separate circuits required one to control the potential between working and reference electrode (potentiostat) and other to convert the sensor current into voltage.
- All the architectures are based on OPAMP and thus do not take full advantage of integration.
- Architectures are complex and not compact.
- Architectures are power hungry and generate larger noise.
- Reference voltage needs to be generated externally or internally.
- As a results these circuit architectures are not suitable for smart phone and implantable glucose sensor applications.

Table below shows the comparison of different architectures

Table 2-2 Comparison of different architectures

| Architecture | Power consumption | Noise | Complexity |
|---|---|---|---|
| Trans-impedance [30] | ≈4.3mW | N/A | Less |
| Trans-impedance variant [29] | 8.64mW | N/A | More |
| Switched capacitor [10] | 1.1mW | ≈2mVrms | Very complex |

# Chapter 3

## Low Power, Low Noise Compact amperometric circuit architecture

As discussed before circuit architectures for ultra-portable applications like smart-phone and implantable glucose sensors should be compact, less noisy and less power hungry. All the circuit architectures discussed in previous chapter are thus not suitable for these applications. In this chapter novel electronic interfacing circuit for three terminal glucose sensor is proposed. Proposed architecture integrates the function of potentiostat and readout circuit there by reducing the complexity of interfacing circuit. The proposed architecture is much compact consumes low power, generates low noise.

### Specifications

Proposed architecture is fabricated in 0.35µM CMOS process. Process parameters are listed below:

Table 3-1 Process Specifications

| **Parameter** | **Value** |
|---|---|
| VDD | 3.3V |
| Minimum L | 0.35µm |
| PAD size | 81.4µm*81.4µm |
| Resistance | 1KΩ/square |
| Metal Layers | 4 |

Process uses 3.3V as power supply while minimum channel length for transistors is 0.35µm. There are several resistors available in the process; the resistor used in this design has sheet resistance of 1KΩ/square. There are total four metal layers available for

interconnections and the pads of size 81.4µm*81.4µm are available to make electrical contact with external world.

Circuit specifications are listed in table below:

Table 3-2 Circuit Specifications

| **Parameter** | **Value** |
|---|---|
| Glucose level | 2.5mM-10mM |
| Sensor current | 6µA-60µA |
| Reference voltage | ≈600mV |
| Output Voltage | 0.13V-1.2V |
| Power Supply | 3.3V |
| Power, noise, area | minimize |

This architecture can be used for detecting glucose levels in blood. Thus it should be able to detect 2.5mM to 10mM of glucose concentration there by covering all three conditions of Hypoglycemia (below 4mM), Euglycemia (4mM-7mM) and hyperglycemia (above 7mM). Corresponding sensor current is around 6 to 60µA. Reference voltage required for glucose sensors varies between 0.2-0.8V for this work we have chosen reference voltage around 0.6V. Output voltage thus varies between130mV to 1.2V. Circuit uses power supply of 3.3V. Main design goal is to minimize power consumption, noise and area.

Proposed Architecture

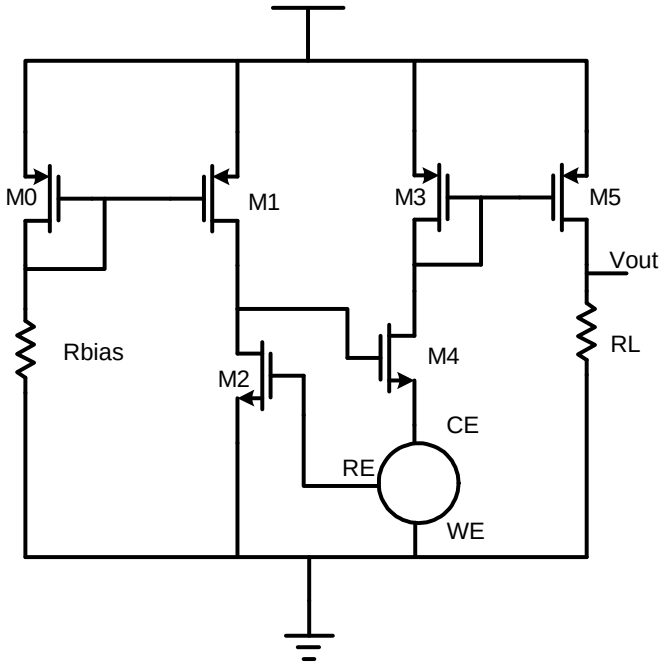


Figure 3-1 Proposed Architecture

Figure 3-1 shows the proposed architecture. It is based on threshold voltage referenced current source [31]. Transistor M1, M2 and M4 forms threshold voltage referenced current source with M1 supplying the reference current. Size of transistor M2 is adjusted such that its gate to source voltage ($V_{GS}$ ) is equal to the threshold voltage. Reference electrode (RE) is connected to the gate of M2 which maintains the constant voltage equal to $V_t$, counter electrode is connected to the source of M2 and working electrode (WE) is grounded. The idea behind this proposed architecture is to use the threshold voltage of a transistor as a reference voltage. Threshold voltage of 0.35µm CMOS process is around 0.6V. Thus threshold voltage of M2 serves as reference voltage and as a result there is no need to supply reference voltage externally. Also reaction current is routed to load resistor RL by current mirror M3 and M5. It can be seen that

proposed architecture effectively integrates the functions of potentiostat and current readout circuit there by making it very compact architecture. Also working electrode is connected to actual ground thus environmental noise pick up is eliminated. In idle state when sensor is not connected, bias current flows only in transistors M0, M1 and M2 thus saving power. Also noise is contributed to output by only transistors M4, M3 and M5 thus making it low noise solution. Advantages of proposed architectures are listed below

- Threshold voltage is used as a reference voltage there by eliminating the need to generate the reference voltage
- Current is routed to output my current mirror configuration
- Architecture effectively integrates the functions of potentiostat and current readout circuit
- No operational amplifiers are required there by making circuit very compact, in other words architecture fully appreciates the power of integrated circuit and presents a customized solution than a general one
- In idle state power is consumed by bias current of four transistor which is very small
- Output noise is contributed by only three transistors thus making it low noise solution
- Working electrode is connected to actual ground there by eliminating environmental noise pickup

Working of this circuit can be better explained by threshold voltage referenced current source.

*Threshold voltage referenced current source*

Figure 3-2 shows the threshold voltage referenced current source. Threshold voltage referenced current source is similar to the Wilson current source with a diode connected transistor replaced by resistor R. Idea behind these type of current source is to generate the bias current depending on voltage other than the supply voltage.

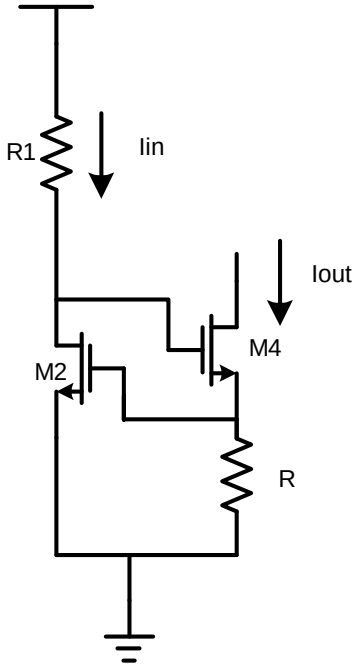


Figure 3-2 Threshold voltage referenced current source

It can be seen that bias current $I_{OUT}$ is nothing but current flowing through resistor R. Equation (3.1) gives the relationship between $I_{OUT}$ and R.

$$I_{OUT} = \frac{V_{GS2}}{R} \tag{3.1}$$

Input current $I_{in}$ is given by following expression

$$I_{in} = \frac{\mu_n C_{ox}}{2}\left(\frac{W}{L}\right)_2 (V_{GS2} - V_t)^2 \tag{3.2}$$

Where $\mu_n$ is electron mobility, $C_{ox}$ is oxide capacitance, (W/L) is the ratio of transistors width and length, $V_t$ is the threshold voltage of transistor. Expression for gate to source voltage of transistor M2 can be obtained from equation (3.2) and is shown below

$$V_{GS2} = V_t + \sqrt{\frac{I_{in}}{\frac{\mu_n C_{ox}\left(W/L\right)_2}{2}}} \tag{3.3}$$

Substituting (3.3) into (3.1) we get

$$Iout = \frac{V_t + \sqrt{\frac{Iin}{\frac{\mu_n C_{ox}\left(W/L\right)_2}{2}}}}{R} \tag{3.4}$$

If the input current is small and $(W/L)_2$ is large such that expression in square root is much smaller than $V_t$ then we can ignore it resulting in following expression

$$Iout \approx \frac{V_t}{R} \tag{3.5}$$

Output impedance of this circuit can be calculated by a small signal model shown in Figure 3-3 and is given by equation (3.6) assuming $gm_2$=$gm_4$=1/R.

$$Rout = ro4 * (2 + gm4 * (ro3 \| R1)) \quad (3.6)$$

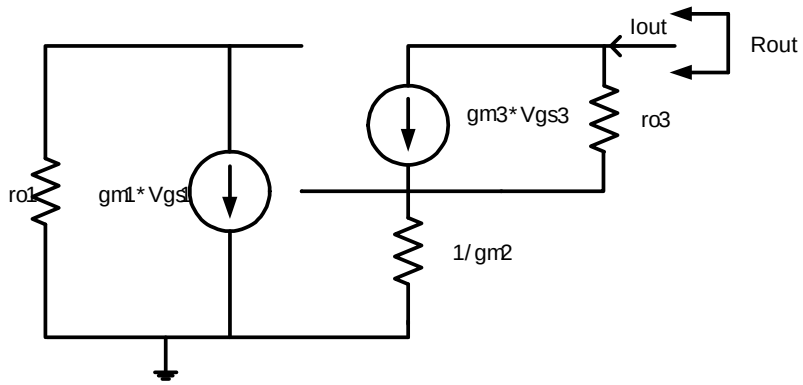


Figure 3-3 small signal model

It can be seen from equation (3.5) that output current varies as value of resistor R varies since $V_t$ is constant. Let see how we can use this idea in out proposed architecture. Figure 3-4 shows the proposed architecture with sensor model.

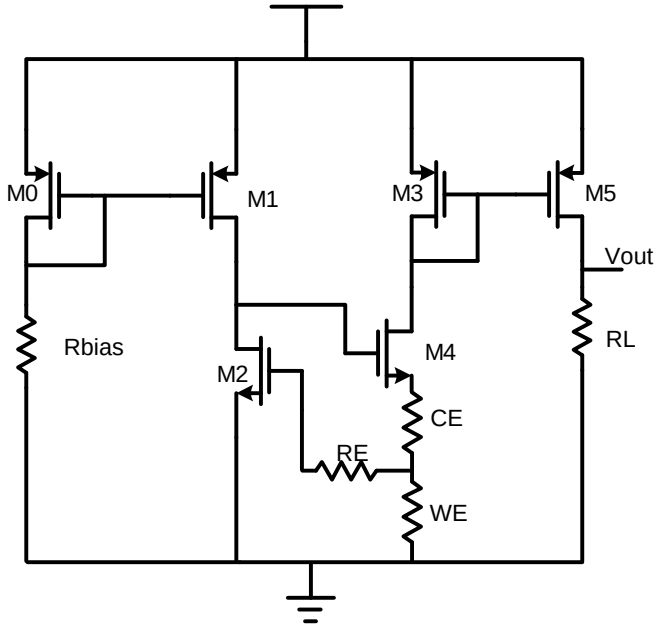


Figure 3-4 Proposed architecture with sensor model

Solution resistances and double layer capacitances are omitted for sake of brevity. Potentiostat maintains constant potential at reference electrode. As resistance of working electrode changes, because of change in glucose concentration, current flowing through the resistance changes this current flow through transistor M4 and is then mirrored by transistor M3 into transistor M5. Transistors M3 and M5 have equal widths thus output current is same as current flowing through M3 and M4.Thus output voltage is given by expression (3.8). It can be seen that as glucose concentration increases working electrode resistance decreases which increases sensor current and thus output voltage.

$$Vout = Iout * R_L \tag{3.7}$$

$$Vout = \left(\frac{V_t}{R_{WE}}\right) * R_L \tag{3.8}$$

*Noise Analysis*

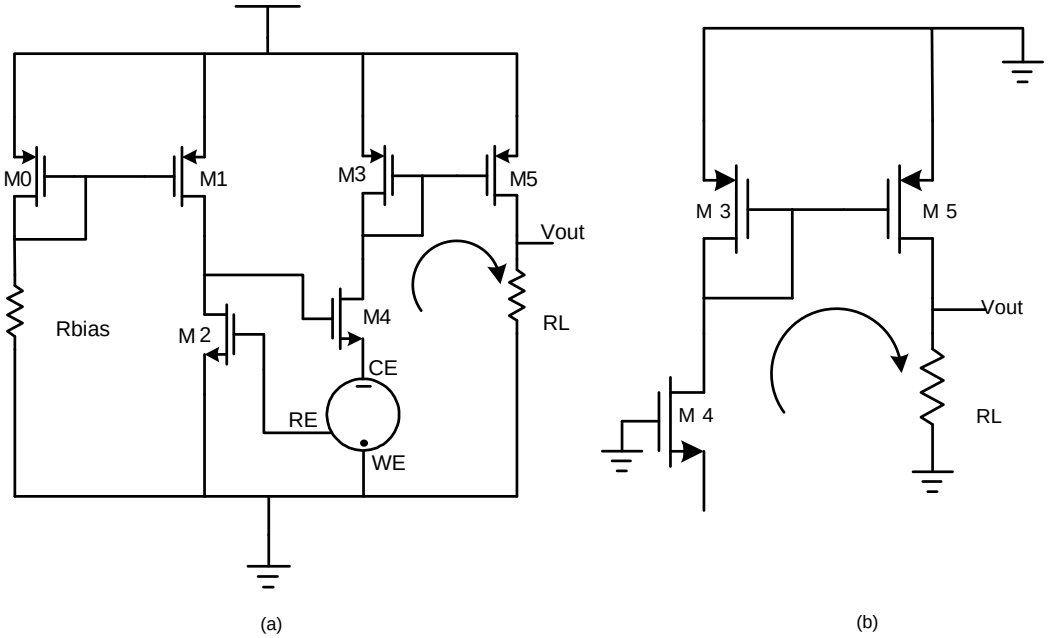


Figure 3-5 (a) Output current path (b) Noise equivalent circuit

**Error! Reference source not found.** (a) shows the path for output current. Output current flows from the transistor M4, M3 and M5 thus these transistors contribute to the noise at output. **Error! Reference source not found.** (b) shows the equivalent circuit for noise analysis. Since noise is a small signal, large signal sources are grounded. Before we analyze the noise in this circuit lets first understand major sources of noise

Thermal Noise also called as Johnson noise is a result of random movement of electrons. It is modeled by a noise current in parallel with the resistor as shown in Figure 3-6 and given by expression (3.8), where K is the Boltzmann constant and T is the temperature in Kelvins. It can be seen by expression noise current can be decreased by increasing the resistance.

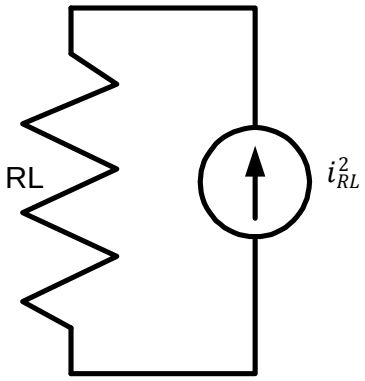


Figure 3-6 Resistor Noise

$$\overline{i_{RL}{}^2} = \frac{4KT}{RL} \tag{3.8}$$

MOSFETs have two main noise sources namely thermal noise of transistor channel and flicker noise or sometimes referred as (1/f) noise. Channel thermal noise [32] is modeled similar to the resistor noise and is given by following expression, where, as before, K is the Boltzmann constant and T is the temperature in Kelvins. (γ, gamma) is the technology constant and varies with the process nodes.

$$\overline{i_{dthermal}{}^2} = \frac{4KT\gamma}{R_{channel}} \tag{3.9}$$

$R_{channel}$ is the channel resistance and is given by following expression, $\mu_n$ is electron mobility, $C_{ox}$ is oxide capacitance, (W/L) is the ratio of transistors width and length, Vgs is the gate to source voltage, $V_t$ is the threshold voltage of MOSFET and gm is the trans-conductance of MOSFET.

$$R_{channel} = \frac{1}{\mu_n C_{ox}\left(W/L\right)\left(V_{gs} - V_t\right)} = \frac{1}{gm} \tag{3.10}$$

Substituting (3.10) in (3.9) gives,

$$\overline{i_{dthermal}}^2 = 4KT\gamma gm \tag{3.11}$$

It can be seen from the equation (3.11) that channel thermal noise is directly proportional to the trans-conductance of the device. Another form of noise that is presents in Mos devices is called flicker noise. Flicker noise is caused because of dangling or incomplete bonds between Silicon and silicon-dioxide interface. Flicker noise is given by following equation:

$$\overline{i_{dflicker}}^2 = \frac{K_f}{C_{ox}W.L}.\frac{1}{f}.gm^2 \tag{3.12}$$

It can be seen from the expression that flicker noise has frequency dependence unlike thermal noise. Flicker noise decrease as frequency increases. In this particular application where signal vary slowly or in other words signal frequency is small flicker noise is very important. Both thermal noise and flicker noise are modeled by a drain current source as shown in Figure 3-7 and total noise current in MOS transistor is given by following expression

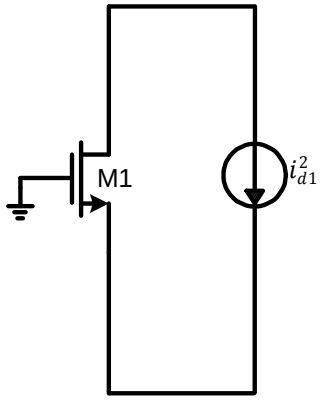


Figure 3-7 MOSFET Noise model

$$\overline{i_a{}^2} = 4KT\gamma gm + \frac{K_f}{C_{ox}W.L}.\frac{1}{f}.gm^2 \quad (3.13)$$

Figure 3-8 shows the simplified schematic for noise analysis [11]. Total output noise voltage is given by equation (3.14). It can be seen from the equation that total output noise current can be reduced by lowering trans-conductance of the transistors. Flicker noise contribution can further be reduced by increasing the transistor length. For this reason length of transistors in this design are kept at 1µm.

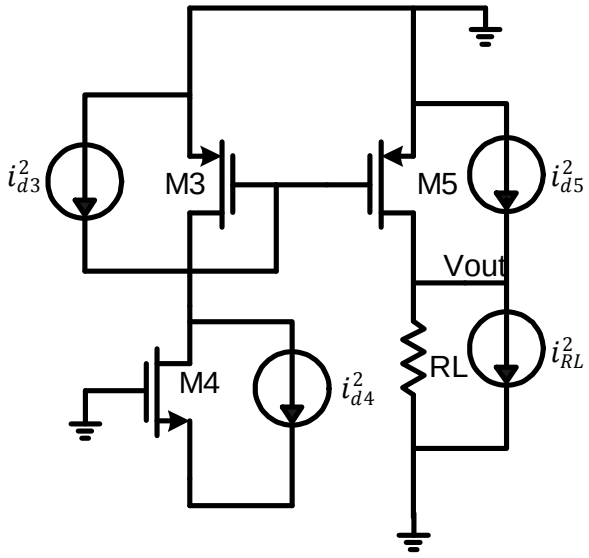


Figure 3-8 Simplified Noise model of proposed architecture

$$\overline{i_{out}{}^2} = \overline{i_{d4}{}^2} + \overline{i_{d3}{}^2} + \overline{i_{d5}{}^2} + \overline{i_{RL}{}^2}$$

$$\overline{i_{out}{}^2} = 4KT\gamma(gm_4 + gm_3 + gm_5) + \frac{K_f}{C_{ox}.f.L}\left(\frac{gm_4{}^2}{W_4} + \frac{gm_3{}^2}{W_3} + \frac{gm_5{}^2}{W_5}\right) + \frac{4KT}{RL} \quad (3.14)$$

$$\overline{v_{out}{}^2} = \overline{i_{out}{}^2} R_L{}^2$$

*Power Supply Dependence*

Ideally output current should reflect the glucose concentration. Thus output current should only change if the glucose concentration is changed. But in reality output current can change because of variety of reasons. Fluctuation in power supply is one of the most important reasons. As results it is important to evaluate the sensitivity of output

current on power supply. Figure 3-9 shows the schematic used to evaluate the power supply dependence. $I_{out}$ is the output current while $I_{in}$ is the input reference current. Sensor model is replaced by Rwe, working electrode resistance

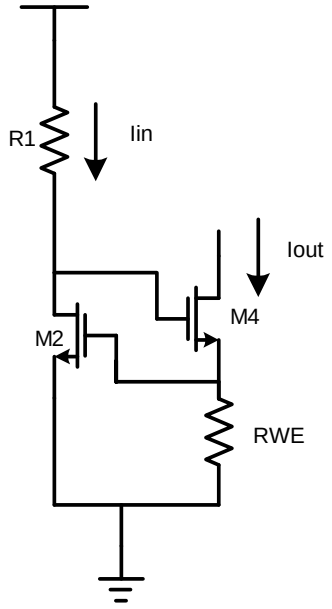


Figure 3-9 Power supply dependence

Sensitivity of output current on power supply (VDD) is given by following equation[31]

$$S_{VDD}^{Iout} = \frac{VDD}{Iout}\frac{\partial Iout}{\partial Vdd} \tag{3.15}$$

Substituting $I_{out}$ from equation (3.4) in (3.15) gives following expression

$$S_{VDD}^{Iout} = \frac{VDD}{Iout} \frac{\partial \left( \frac{V_t + \sqrt{\frac{2.I_{in}}{\mu_n C_{ox}\left(W/L\right)_2}}}{R_{WE}} \right)}{\partial Vdd} \tag{3.16}$$

$$S_{VDD}^{Iout} = \frac{VDD}{Iout} . \frac{1}{2.R_{WE}} . \frac{1}{\sqrt{\frac{2.I_{in}}{\mu_n C_{ox}\left(W/L\right)_2}}} . \frac{2}{\mu_n C_{ox}\left(W/L\right)_2} . \frac{\partial Iin}{\partial Vdd} \tag{3.17}$$

$$S_{VDD}^{Iout} = \frac{1}{Iout} . \frac{1}{2.R_{WE}} . \frac{1}{\sqrt{\frac{2.I_{in}}{\mu_n C_{ox}\left(W/L\right)_2}}} . \frac{2}{\mu_n C_{ox}\left(W/L\right)_2} Iin. \frac{VDD}{Iin} . \frac{\partial Iin}{\partial Vdd} \tag{3.18}$$

$$S_{VDD}^{Iout} = \frac{1}{Iout} . \frac{1}{2.R_{WE}} . \frac{1}{\sqrt{\frac{2.I_{in}}{\mu_n C_{ox}\left(W/L\right)_2}}} . \frac{2}{\mu_n C_{ox}\left(W/L\right)_2} Iin. \frac{VDD}{Iin} . \frac{\partial Iin}{\partial Vdd} \tag{3.19}$$

Since,

$$V_{ov2} = \frac{2}{\mu_n C_{ox}\left(W/L\right)_2} Iin \tag{3.20}$$

Substituting (3.20) in (3.19) gives

$$S_{VDD}^{Iout} = \frac{V_{ov2}}{Iout} . \frac{1}{2.R_{WE}} . S_{VDD}^{Iin} \ , S_{VDD}^{Iin} \approx 1 \tag{3.21}$$

As $V_{gs2} = I_{out} * R_{WE}$ , final expression for sensitivity of output current on power supply is given by following equation

$$S_{VDD}^{Iout} = \frac{V_{ov2}}{2.V_{gs2}}$$
$$V_{ov2} = V_{gs2} - V_t \approx 0 \quad (3.22)$$
$$S_{VDD}^{Iout} \approx 0$$

It can be seen from the analysis that output current is independent of supply voltage.

*Stability Analysis*

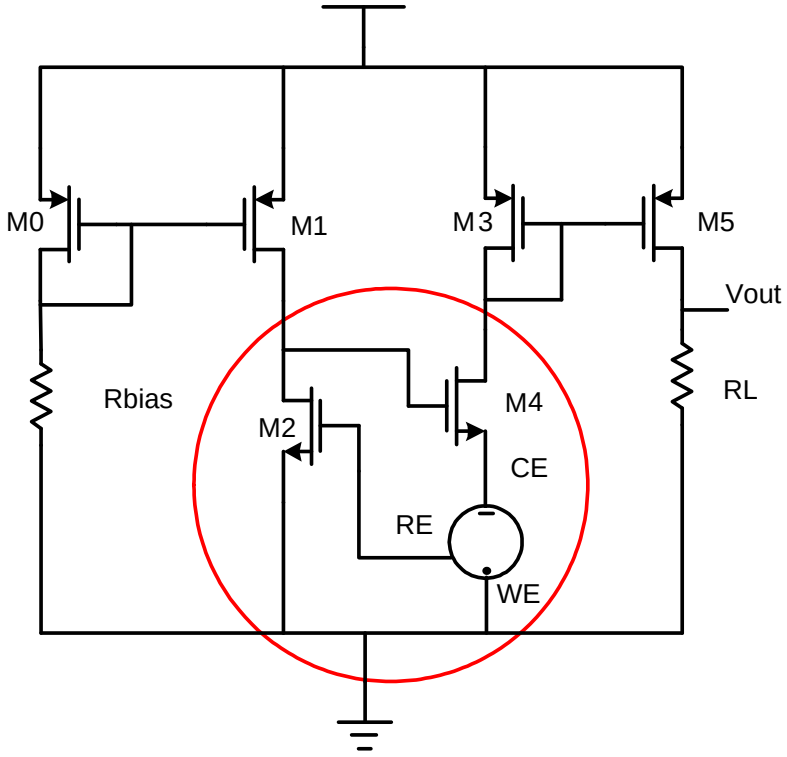


Figure 3-10 Feedback loop formed by transistors and glucose sensor

Even though the input signal is a low frequency signal it is important to evaluate the stability of the circuit because of the feedback formed by transistor M2, M4 and glucose sensor as shown in Figure 3-10 Feedback loop formed by transistors and glucose sensor. Best way to understand the stability of the circuit is to find the loop gain. In order to find the loop gain lets simplify the circuit as shown in Figure 3-11. Biasing network (formed by transistors M0 and M1) and output network (formed by current mirror M3 and M5) is replaced by load (R0, C0 and RL and CL) respectively as they are not part of the feedback network. In final simplification step glucose sensor is replaced by only working electrode resistance $R_{WE}$ because working electrode resistance varies with the glucose concentration. Thus it is necessary evaluate circuit stability as working electrode resistance varies. Also gate to source capacitance (Cgs) of transistor M2 is also included in the model this is because size of transistor M2 is much bigger. Figure 3-12 shows the simplified circuit.

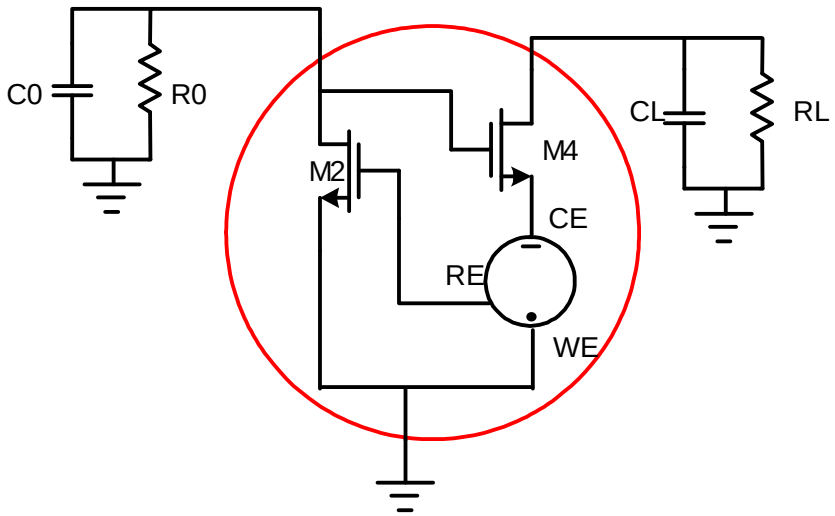


Figure 3-11 Small signal model for stability analysis

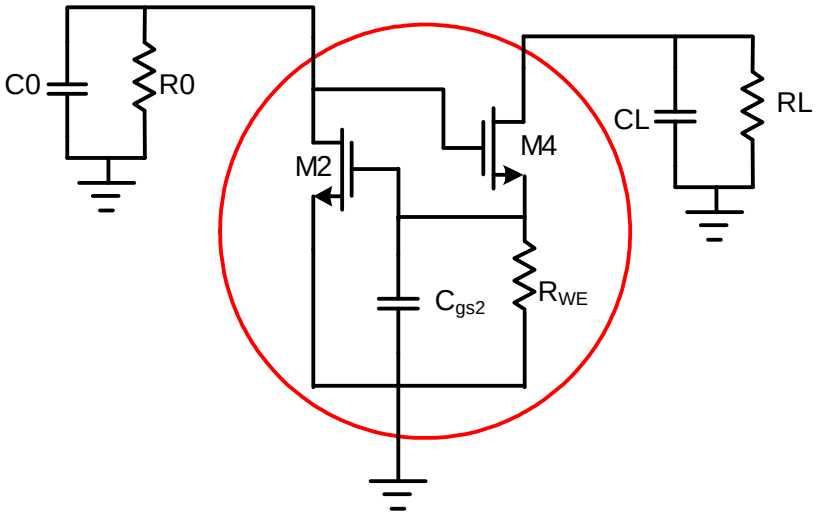


Figure 3-12 Replacing glucose sensor

In the next step transistors M2 and M4 are replaced by small signal models as shown in Figure 3-13. Small signal shown thus contains all the important parameters that can affect the stability.

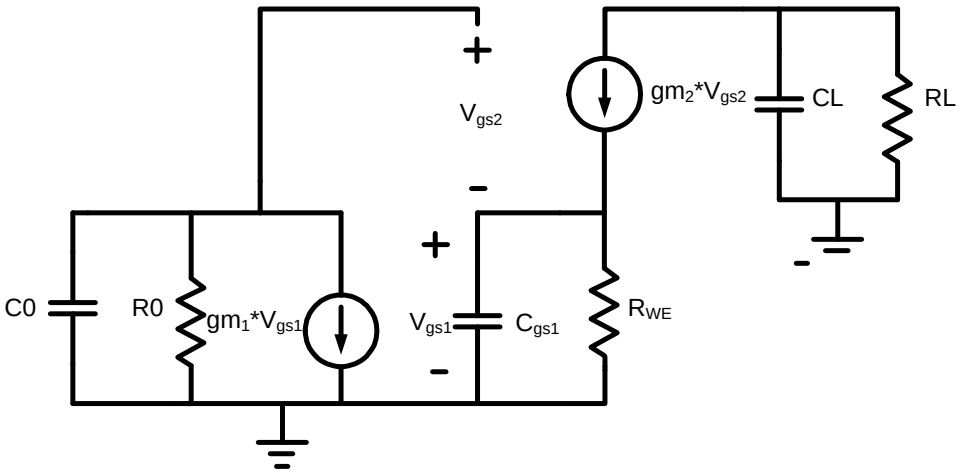


Figure 3-13 Complete small signal model for stability analysis

To evaluate the loop gain we have to break the loop, insert the test voltage and evaluate the transfer function around the loop as shown in Figure 3-14. This analysis is also referred to as return ratio analysis.

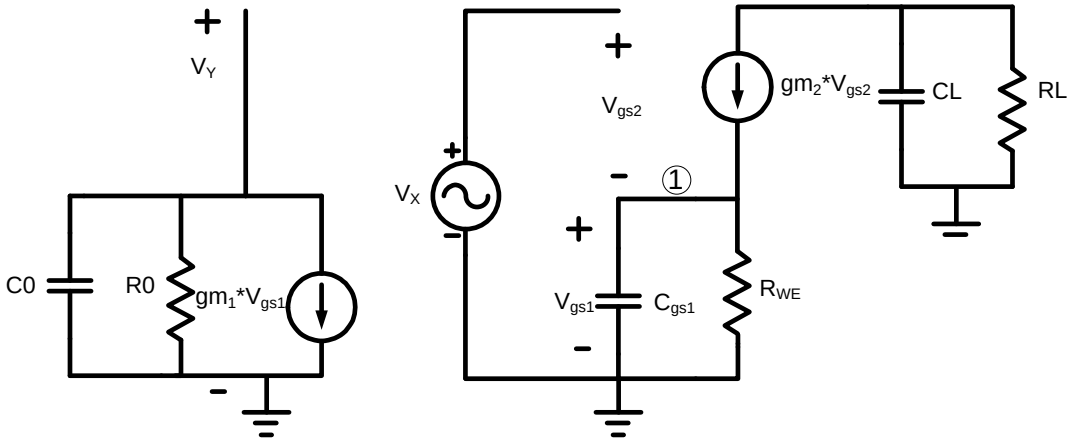


Figure 3-14 Return ratio analysis

Loop gain is then can be defined as the ratio of voltage at node $V_Y$ to voltage at node $V_X$ as given in following equation

$$Loop\ Gain\ (LG) = \frac{V_Y}{V_X} \tag{3.23}$$

Applying Kirchoof's current law (KCL) at node 1 in Figure 3-14 we get,

$$V_{gs1} = gm_2.V_{gs2}.\left(\frac{R_{WE}}{1 + s.C_{gs1}.R_{WE}}\right) \tag{3.24}$$

While $V_{GS2}$ can be found by subtracting $V_X$ from $V_{GS1}$ as shown in following expression

$$V_{gs2} = V_X - V_{gs1} \tag{3.25}$$

Substituting (3.25) in (3.24) gives,

$$V_{gs1} = \frac{gm_2.V_X.\left(\frac{R_{WE}}{1+s.C_{gs1}.R_{WE}}\right)}{1+gm_2.\left(\frac{R_{WE}}{1+s.C_{gs1}.R_{WE}}\right)} \tag{3.26}$$

Voltage at node VY can be found by applying KCL at that node

$$V_Y = -gm_1.V_{gs1}.\left(\frac{R0}{1+s.C0.R0}\right) \tag{3.27}$$

Substituting (3.26) in (3.27) gives the expression for loop gain

$$Loop\ gain(LG) = \frac{V_Y}{V_X} = -gm_1.R0.\left(\frac{1}{(1+s.R0.C0)\left(1+\frac{s.C_{gs1}.R_{WE}}{1+gm_2.R_{WE}}\right)}\right) \tag{3.28}$$

It can be seen from the transfer function for loop gain (3.28) system has two poles as shown in equation (3.29)

$$\omega_{p1} = -\frac{1}{R0.C0}$$
$$\omega_{p2} = -\frac{1+gm_2.R_{WE}}{C_{gs1}.R_{WE}} \approx -\frac{gm_2}{C_{gs1}} \approx \omega_T \tag{3.29}$$

It can be seen that $\omega_{p1}$ is the dominant pole since $\omega_{p2}$ equals to the transition frequency of the transistor which is much higher. Also $\omega_{p2}$ does not depend on the working electrode resistance. Thus circuit is unconditionally stable for all working electrode resistances.

*Simulation Results*

Proposed architecture is designed in CMOS 0.35um technology. Circuit is laid out in Cadence and then parasitic extractions are done to obtain parasitic resistance and capacitances. Figure 3-16 shows the layout of complete chip. Circuit marked as A is the proposed architecture. Figure 3-16 shows the layout of proposed architecture. Layout occupies 125µm*340µm of area. Post extracted layout is used to carry out simulations. Circuit is simulated with electrical model of sensor. Simulation results are shown in Figure 3-17. It can be seen that output voltage varies from 0.13V-1.2V for sensor current 6µA-60µA. Simulation results show very linear response. Linearity is important performance criterion as it decides the accuracy of the circuit.

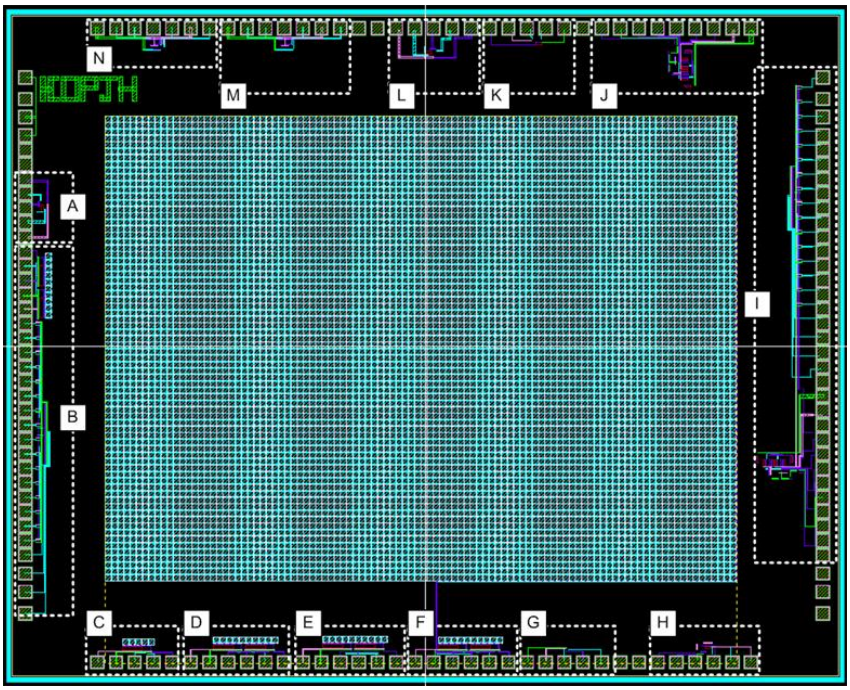


Figure 3-15 Full Chip Layout

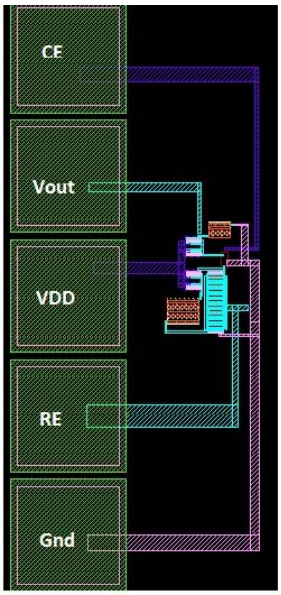


Figure 3-16 Layout of proposed architecture

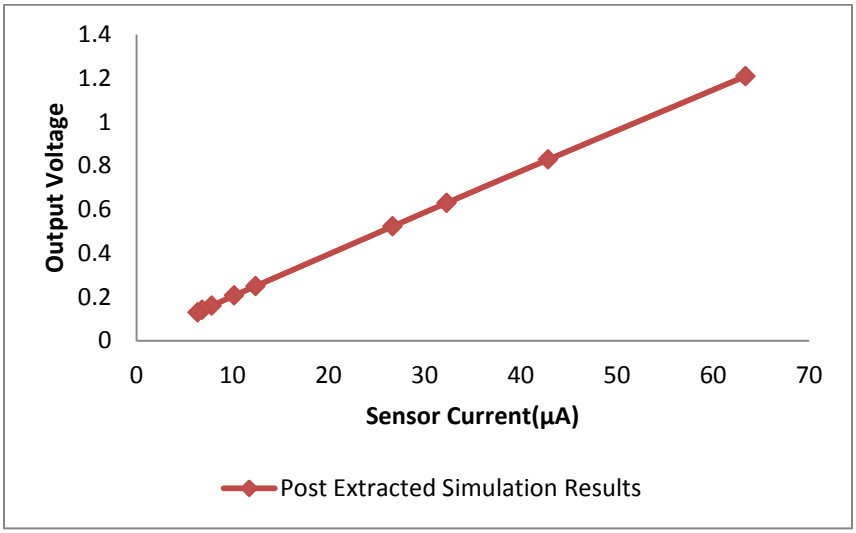


Figure 3-17 Post extraction simulations

Figure 3-18 shows the noise simulation results. Noise is simulated up to 100MHz bandwidth. It can be seen at lower frequencies flicker noise dominates while as frequency increases thermal noise dominates. Frequency at which flicker noise power equals to that of thermal noise power is called corner frequency. Total integrated noise in 0-100Hz bandwidth is 0.348µVrms while noise integrated in 100MHz bandwidth is 298.379µVrms. Integrated noise suggests the minimum signal that can be detected by the system. Lower the noise higher the sensitivity of the system.

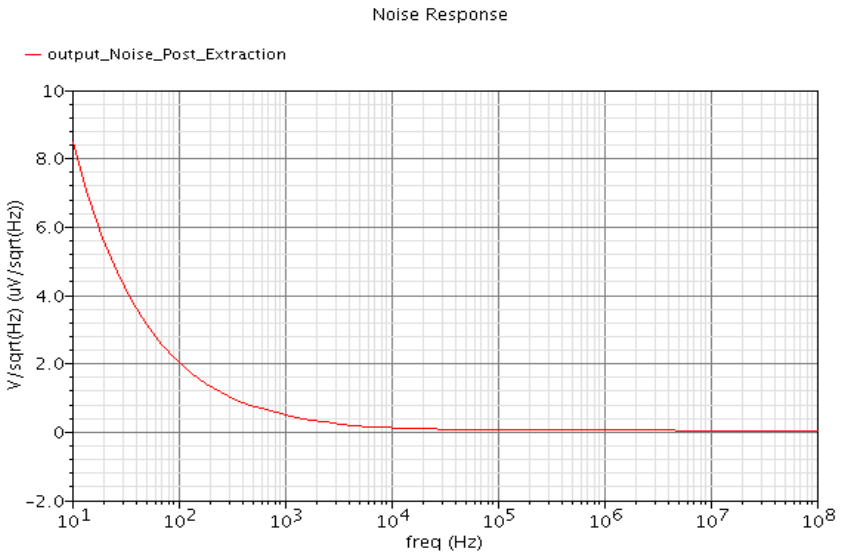


Figure 3-18 Noise Simulation

Figure 3-19 shows the bode plot used for the stability analysis. Phase margin when sensor current is 6µA is $48.44^0$ while phase margin when sensor current is 60µA is $46.44^0$. Thus it can be seen that circuit is stable for all sensor currents in other words for all the working electrode resistances. Following table summarizes the simulation results.

Table 3-3 Post extraction simulation results

| **Parameter** | **Post extraction simulation** |
|---|---|
| Output voltage | 0.13V-1.2V |
| Total integrated noise | 298.379µVrms (100MHz BW) |
| Power dissipation | 136.85µW |

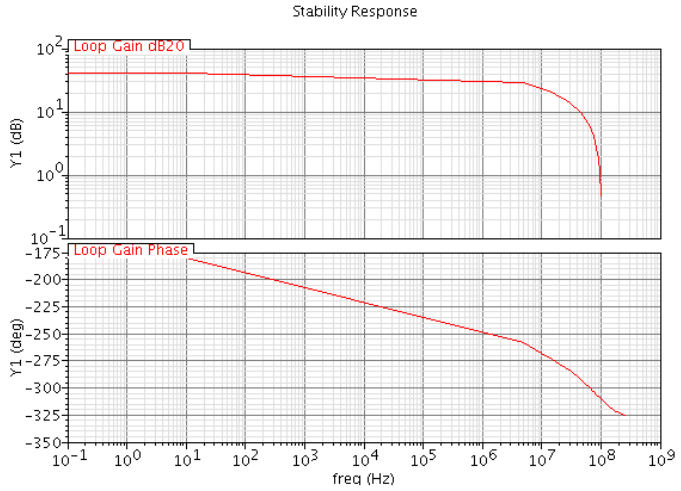


(a)

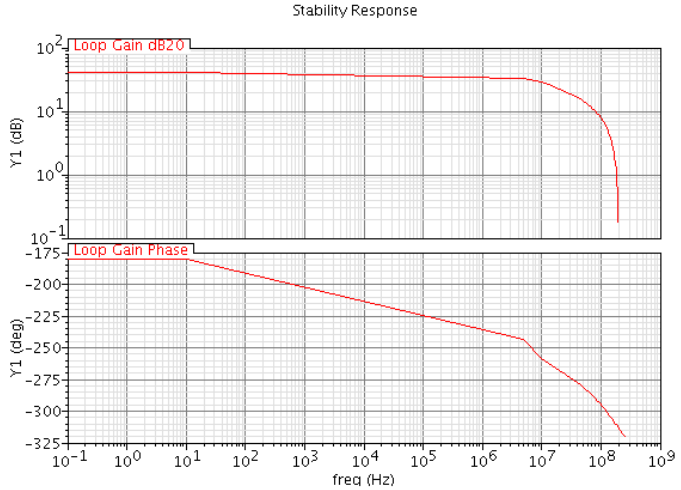


Figure 3-19 (a) Bode plot for sensor current 6µA (b) bode plot for sensor current 60µA

*Measurement Results*

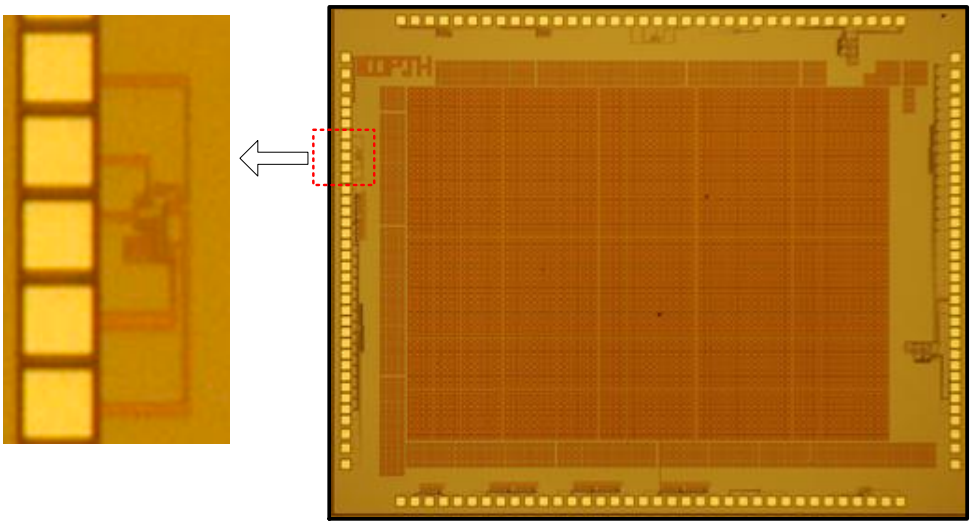

Figure 3-20 Die Photograph

Figure 3-20 shows the die photograph of fabricated chip. Fabricated chip is then packaged and Figure 3-21 shows the photograph of packaged chip, quad flat package is used for packaging. In order to test the chip firstly a chip socket is soldered on to the adapter board as shown in Figure 3-22. Chip is then put in the socket. Sensor model is assembled on the bread board and connections are made from adapter board to bread board. Figure 3-23 shows the measurement setup. Keithley 2400 source-meters are used to measure sensor current and output voltage. Agilent power supply is used to power on the chip. Measurement results are shown in Figure 3-24 .Measurement results show very linear response. Linearity is important performance criterion as it decides the accuracy of the circuit. Measurement and simulation results are plotted together in Figure 3-25 for comparison purpose.


Figure 3-21 Photograph of packaged chip

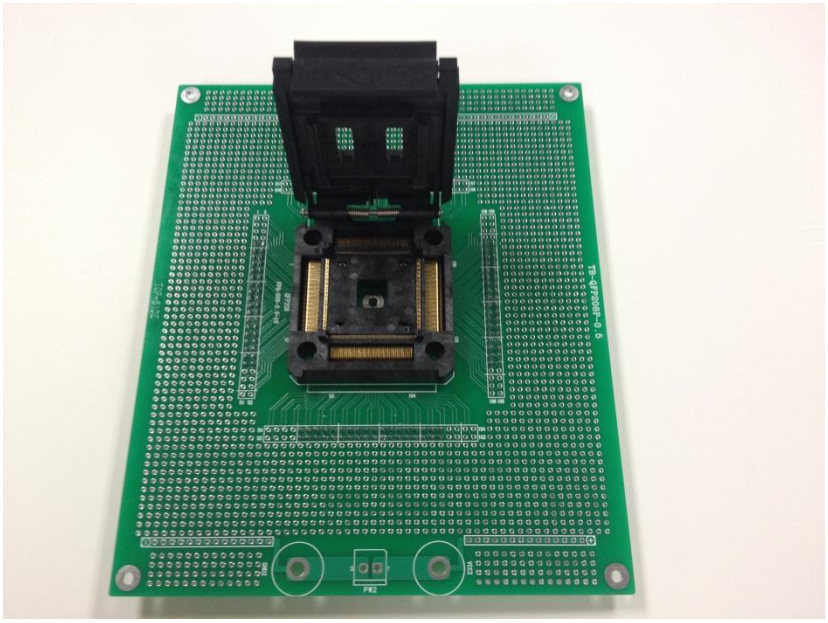

Figure 3-22 Adapter board with socket

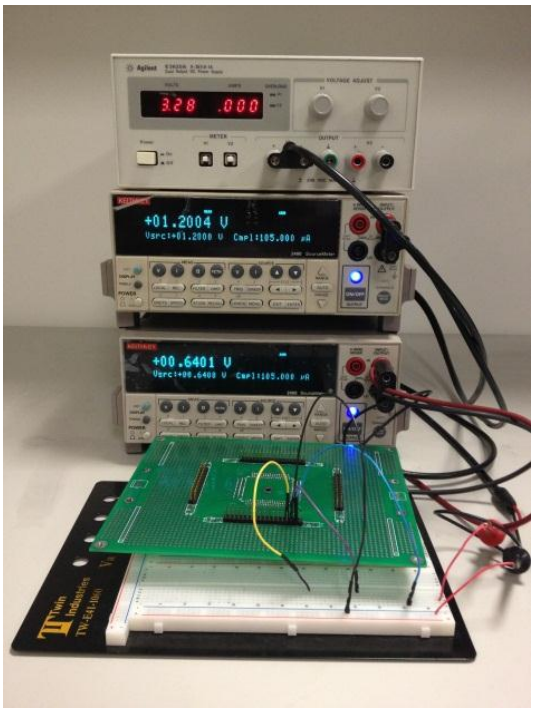


Figure 3-23 Measurement Setup

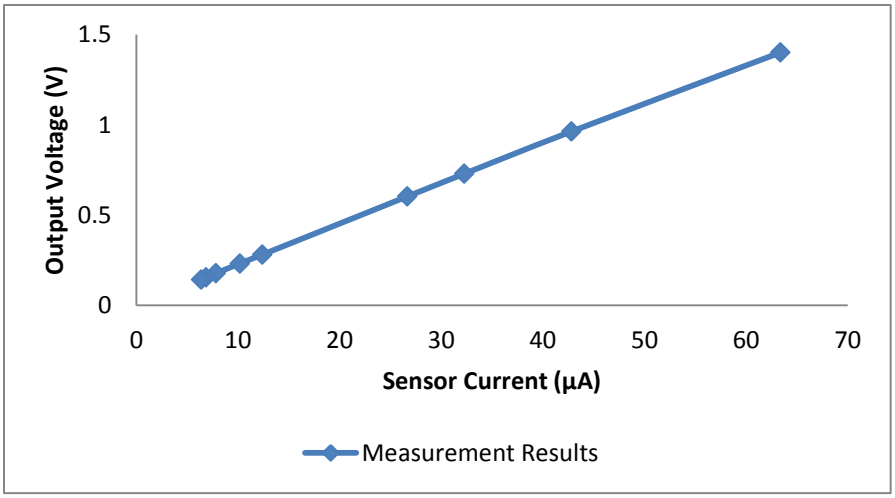


Figure 3-24 Measured results

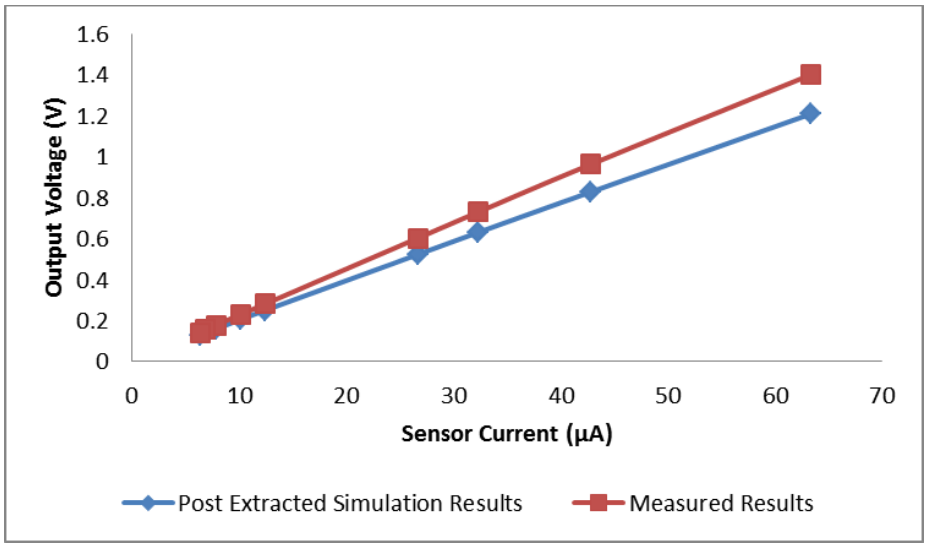


Figure 3-25 Comparison of measured and simulated results

It can be seen that measured and simulated results closely match. Maximum error between simulation and measurement results is 15%. Error occurs mainly because of chip parasitic and packaging parasitic. Also fabrication process induces certain mismatches between the components (for example in transistor lengths and width can vary, exact value of resistor can vary). Figure 3-26 shows the noise measurement results. Noise is measured with the help of oscilloscope. Since oscilloscope measured the transient or time domain vales, RMS values are used to measure the noise. Total noise thus measured is around 312µVrms. Result closely matches with the simulation and suggests the minimum signal that can be detected by the system. Lower the noise higher the sensitivity of the system.

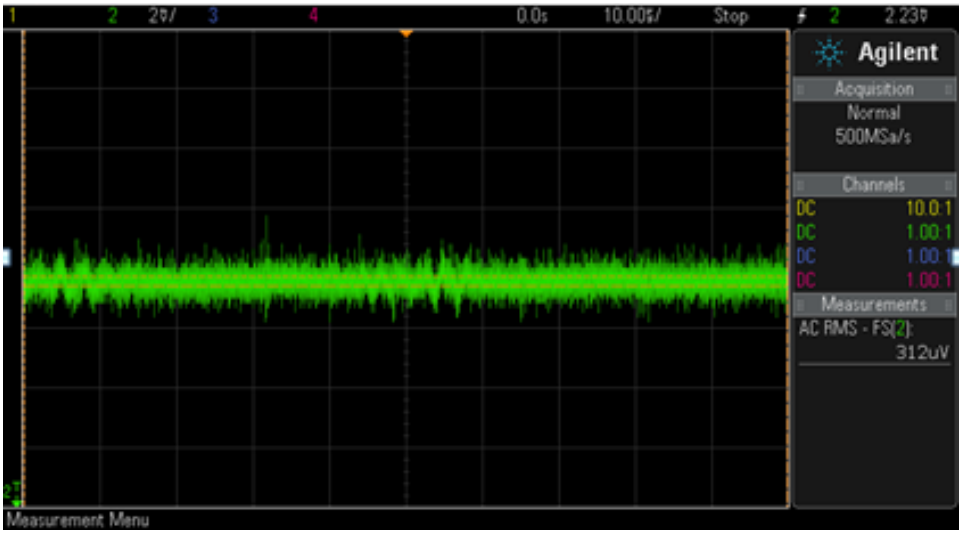


Figure 3-26 Noise Measurement

Table 3-4 shows the comparison between simulations and measurement results. It can be seen that measurement results closely match simulation results. Result also show that important performance criterions (like low power, low noise and compactness) for ultraportable glucose sensing applications like smart phone integration and implantable glucose sensing are met by this novel architecture.

Table 3-4 Comparison between measurement and simulation results

| **Parameter** | **Post extraction simulation** | **Measurement** |
|---|---|---|
| Output voltage | 0.13V-1.2V | 0.14V-1.4V |
| Total integrated noise | 298.379µVrms (100MHz BW) | 312µVrms (100MHz BW) |
| Power dissipation | 136.85µW | 199µW |

In order to validate the circuit, measurements are done with actual three electrode amperometric glucose sensor. Figure 3-27 shows the measurement setup. Keithley 2400 source-meters are used to measure sensor current and output voltage. Agilent power supply is used to power on the chip. The package chip is put in the socket and pins are interfaced with glucose sensor. For measurements four different concentrations of glucose solution are prepared (2.5, 5, 8,10mM) so as to cover the all the three conditions namely Hypoglycemia (low blood glucose level below 4mM), Euglycemia (normal blood glucose levels 4-7mM) and hyperglycemia (high blood glucose levels above 7mM). In order to make glucose solution 180.16gms of glucose (molecular weight of glucose) is weighed and then mixed into one liter of PBS (phosphate buffer saline) solution. This gives solution of 1M. This solution can then be diluted to make the different concentrations of glucose solution. Three electrode glucose sensors is immersed in the glucose solution and connection are made with the chip. Figure 3-28 shows the measured results.

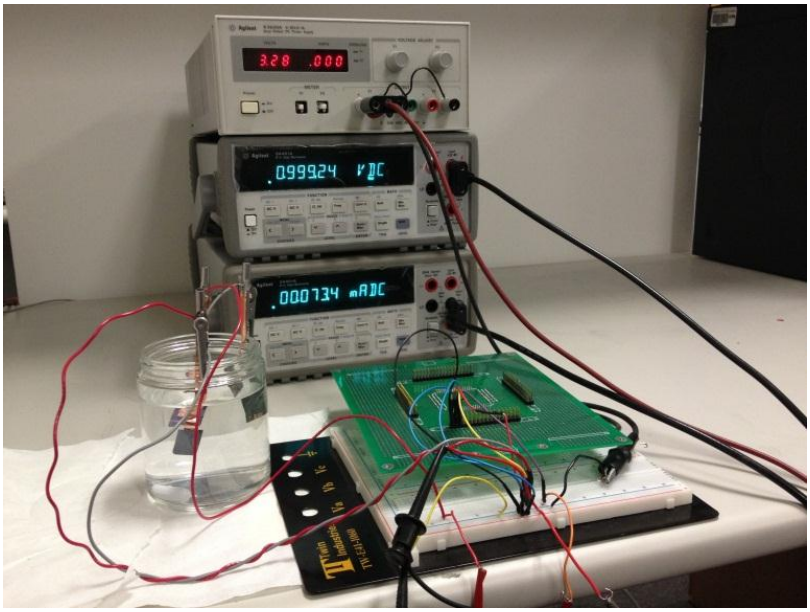

Figure 3-27 Measurement setup with Glucose sensor

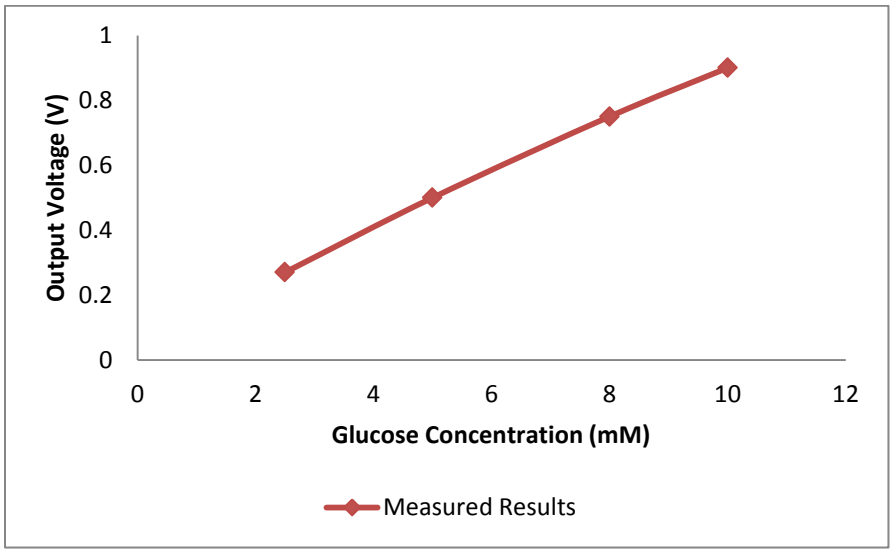


Figure 3-28 Measurement Results with glucose sensor

Results show linear relationship between glucose concentration and output voltage varies from 0.27 to 0.9V for glucose concentration varying from 2.5 to 10mM.

Results show the same trend as compared to the results with sensor model. Linearity shows that different glucose concentrations can be detected uniquely.

Table 3-5 shows the comparison of this work with previous architectures. Power consumed by proposed architecture is 199µW which very small compared to the other architectures. This means that proposed architecture can give greater battery life needed for ultraportable applications. Also noise generated is 312µVrms which means small signals can be detected. It is also shown that output voltage is varies linearly with the glucose concentration.

Table 3-5 Comparison of proposed architecture with previous architectures

| **Architecture** | **Power consumption** | **Noise** | **Complexity** |
|---|---|---|---|
| Trans-impedance[30] | ≈4.3mW | N/A | Less |
| Trans-impedance variant[29] | 8.64mW | N/A | More |
| Switched capacitor[10] | 1.1mW | ≈2mVrms | Very complex |
| This work | 199µW | 312µVrms | Compact |

Thus proposed architecture is more compact, generates less noise and consumes much less power. This architecture is suited for the ultra-portable glucose sensing applications like smart phone integration and implantable glucose sensing.

# Chapter 4

## Wide dynamic range potentiostat architecture for low concentration glucose sensing

Detecting glucose levels from the blood is the most widely used method but other fluids like tear fluid are also used to detect the glucose levels. For detecting glucose levels from blood sample of blood is obtained by pricking the hand and is the invasive method. With advent of MEMS technology semi invasive micronedles are also developed with which pricking is not necessary [33]. Normal blood glucose levels are 4-7mM while people with diabetes have blood glucose levels higher than 7mM,condition called Hyperglycemia or below 4mM, condition called hypoglycemia [34]. Even though sensing glucose concentration from blood is the most popular method it is inconvenient for people who require constant monitoring of glucose levels and frequent pricking may also cause infection. Alternate non-invasive methods like near infrared spectroscopy have also been developed but are not very popular because of challenges of interference and other biochemical and low signal strengths[3]. Sensing glucose concentration from tear fluid is another non-invasive method for glucose detection. Tear fluid is directly accessible on the eye and can be used as a chemical interface between sensor and human body. Different levels of glucose concentrations are reported in tear fluid, it depends on the amount of tear analyzed, and they range from few hundreds of µM to few mM [3][4][5]. For the purpose of this paper we have considered the tear glucose concentration in the range of 1-2mM.

## Specifications

Proposed architecture is fabricated in 0.35µM CMOS process. Process parameters are listed below:

Table 4-1 Process Specifications

| **Parameter** | **Value** |
|---|---|
| VDD | 3.3V |
| Minimum L | 0.35µm |
| PAD size | 81.4µm*81.4µm |
| Resistance | 1KΩ/square |
| Metal Layers | 4 |

Process uses 3.3V as power supply while minimum channel length for transistors is 0.35µm. There are several resistors available in the process; resistor used in this design has sheet resistance of 1KΩ/square. There are total four metal layers available for inter-connections and the pads of size 81.4µm*81.4µm are available to make electrical contact with external world.

Circuit specifications are listed in table below:

Table 4-2 Circuit Specifications

| **Parameter** | **Value** |
|---|---|
| Glucose level | 1mM-10mM |
| Sensor current | 0.6µA-60µA |
| Reference voltage | ≈600mV |
| Output Voltage | 0.13V-1.2V |
| Power Supply | 3.3V |

Architecture is used for detecting glucose levels in blood and in tear fluid. Thus it should be able to detect 2.5mM to 10mM of glucose concentration there by covering all three conditions of Hypoglycemia (below 4mM), Euglycemia (4mM-7mM) and hyperglycemia (above 7mM). Corresponding sensor current is around 6 to 60µA. Also tear glucose levels are between 1mM-2mM which should also be detected by the circuit. Reference voltage required for glucose sensors vary between 0.2-0.8V for this work we have chosen reference voltage around 0.6V. Out voltage thus varies between130mV to 1.2V. Circuit uses power supply of 3.3V. Main design goal is to minimize power consumption, noise and area.

Proposed Architecture

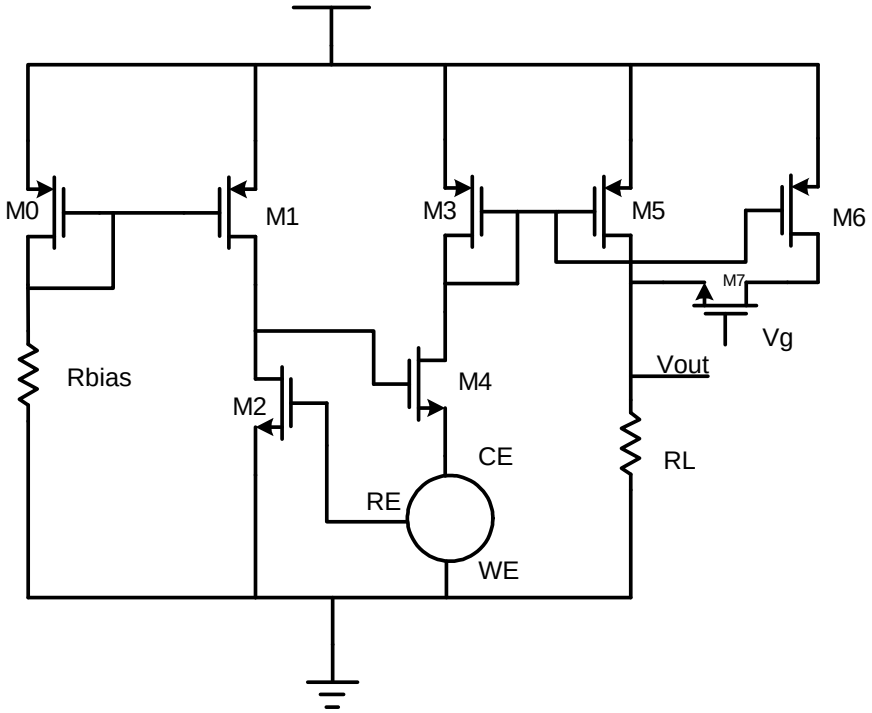


Figure 4-1Proposed architecture for low concentration glucose detection

Figure 4-1 shows the proposed architecture. Architecture is based on threshold voltage referenced current source. Transistor M0 and M1 forms the current mirror and establish reference current for transistor M2. Size of transistor M2 is adjusted such that gate to source voltage of M2 is equal to the threshold voltage. This threshold voltage serves as the reference voltage and is applied to the reference electrode RE. Working electrode is grounded while counter electrode is connected to source of transistor M4. When reaction takes place at working electrode, current proportional to the reaction passes through transistor M4 and is mirrored to transistor M5 and produces the output voltage across load resistor RL. Transistor M6 and M7 serves as variable gain circuit. Width of transistor M6 is nine times greater than that of M5, M6 serves as a switch. Reaction current corresponding to the low concentration of glucose is smaller, in this case switch M7 can be turned on by applying control voltage Vg to gate of M7. The reaction current is now amplified ten times by transistor M5 and M6 and thus produces larger output voltage across load resistor RL. Detailed working of the circuit can be better understood by understanding threshold referenced current source.

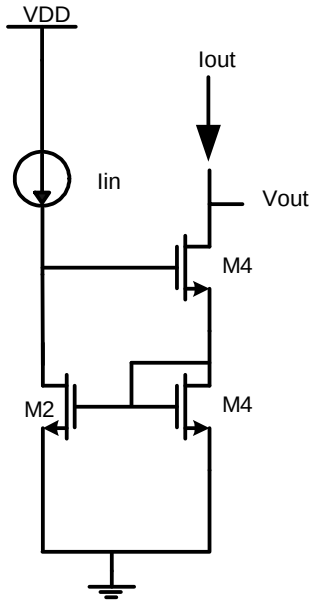


Figure 4-2 Threshold referenced voltage source

Threshold referenced current source, shown in Figure 4-2, is similar to the Wilson current source with a diode connected transistor is replaced by resistor R. Idea behind these type of current source is to generate the bias current depending on voltage other than the supply voltage. It can be seen that bias current $I_{OUT}$ is nothing but current flowing through resistor R. Equation (4.1) gives the relationship between $I_{OUT}$ and R.

$$I_{OUT} = \frac{V_{GS2}}{R} \tag{4.1}$$

Relation between $I_{OUT}$ and threshold voltage $V_t$ can be established as shown in equation (4.2)

$$I_{OUT} = \frac{Vt + V_{ov2}}{R} = \frac{V_t + \sqrt{\frac{I_{in}}{\frac{\mu_n C_{ox}}{2}\left(W/L\right)_2}}}{R} \tag{4.2}$$

$V_{ov2}$ is the overdrive voltage M2, $I_{in}$ is the reference current, $\mu_n$ is the electron mobility, $C_{ox}$ is oxide capacitance and $(W/L)_2$ is ratio of transistor width to length. If reference current $I_{in}$ is sufficiently low and $(W/L)_2$ is large then $I_{OUT}$ depends on the ratio of threshold voltage and resistance R as shown in equation (4.3)

$$I_{OUT} \approx \frac{V_t}{R} \tag{4.3}$$

This architecture is similar to the previous architecture with the exception of transistors M6 and M7 which forms variable gain part of the circuit. Idea is to have a larger gain when detecting low concentration and small gain when detecting a large concentration. The architecture also gives control to select the gain. All other analysis for this architecture are similar to previous architecture and are not repeated here.

*Simulation Results*

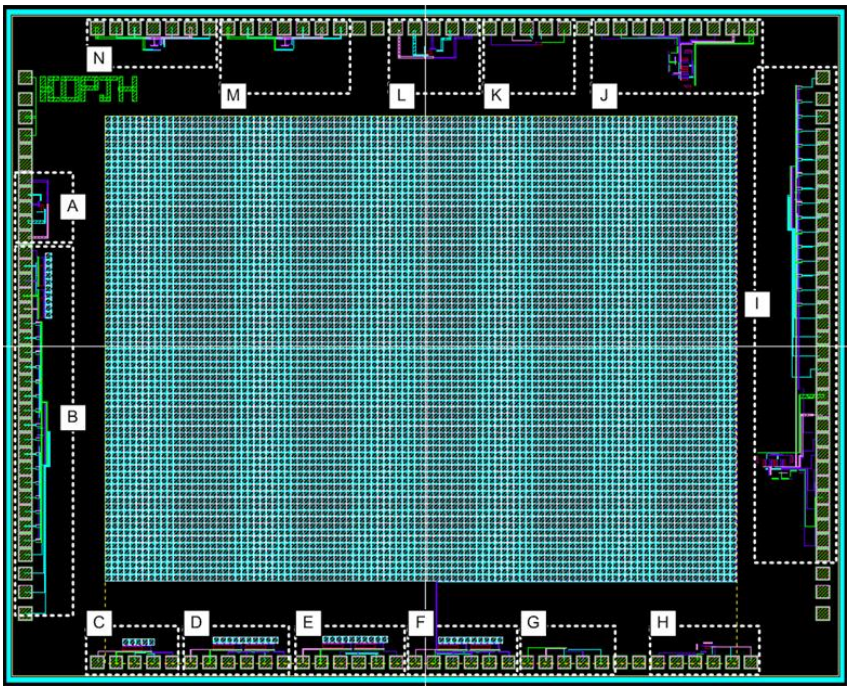


Figure 4-3 Full Chip layout

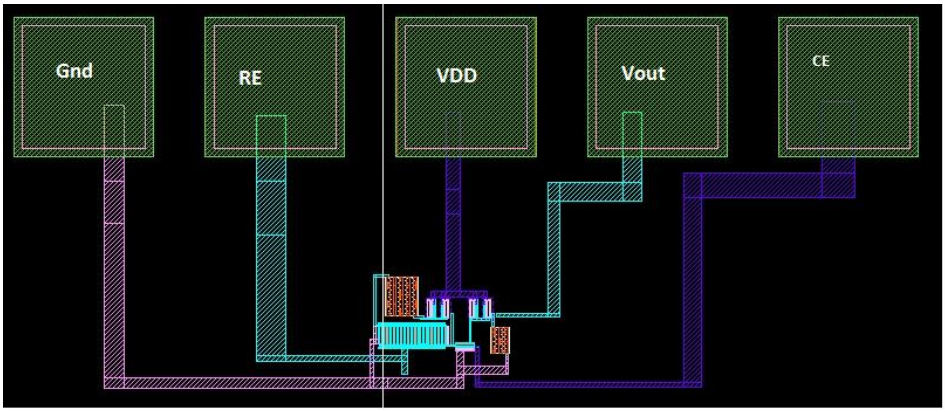


Figure 4-4 Layout of variable gain architecture

Proposed architecture is designed in CMOS 0.35um technology. Circuit is laid out in Cadence and then parasitic extractions are done to obtain parasitic resistance and

capacitances. Figure 4-4 shows the layout of the complete chip. Layout of proposed circuit is marked as H and shown in Figure 4-4. Layout occupies 116µm*551µm of area. Post extracted layout is used to carry out simulations. Circuit is simulated with electrical model of sensor. Simulation results are shown in Figure 4-5. When gate voltage is zero volts then transistor M7 is turned off and the architecture is same as the one discussed in the previous chapter. It can be seen from Figure 4-5(a) that output voltage varies from 0.13V-1.2V for sensor current 6µA-60µA. When gate voltage is high (3.3V in this case) then transistor M7 is turned on and transistor M6 supplies current to the output. Thus even though the sensor current is ten times smaller output voltage is same as shown in Figure 4-5 (b). Simulation results show very linear response. Linearity is important performance criterion as it decides the accuracy of the circuit.

Noise simulation is shown in Figure 4-6. It can be seen at lower frequencies flicker noise dominates while as frequency increases thermal noise dominates. Frequency at which flicker noise power equals to that of thermal noise power is called corner frequency. Total integrated noise in 0-100MHz bandwidth is 430.7µVrms. shows the noise simulation results. Noise is simulated up to 100MHz bandwidth. Integrated noise suggests the minimum signal that can be detected by the system. Lower the noise higher the sensitivity of the system.

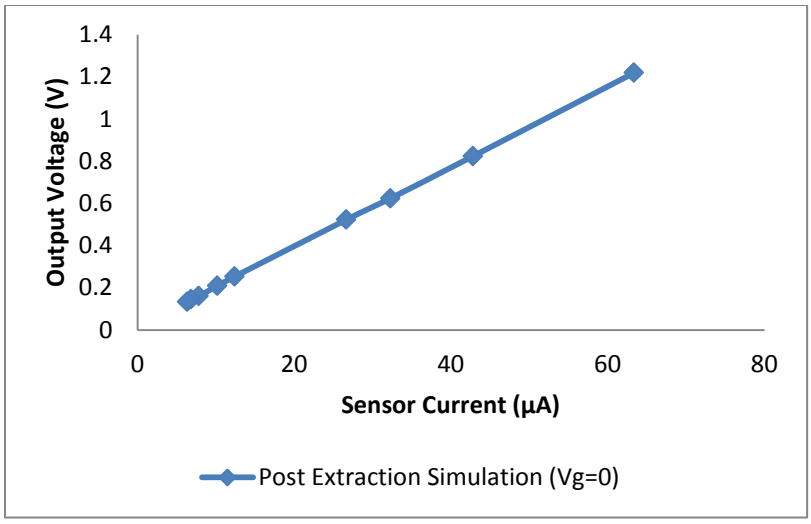


(a)

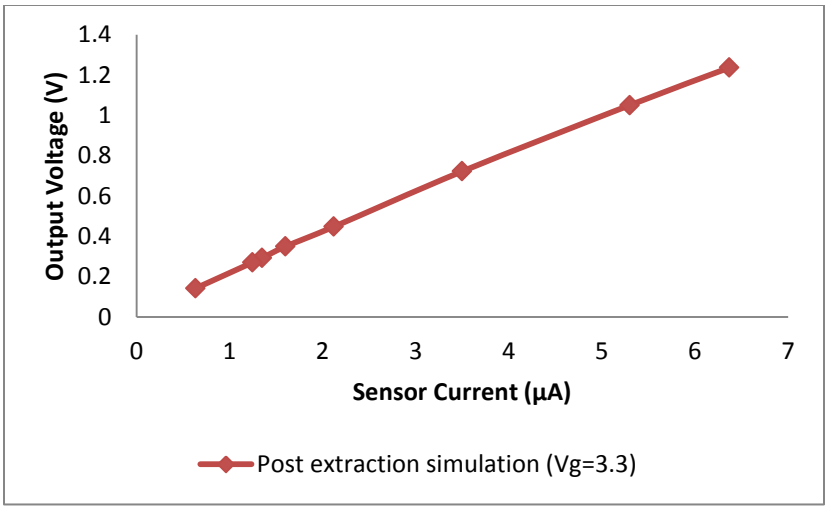


(b)

Figure 4-5 Post extracted simulation (a) Vg=0 (b) Vg=3.3V

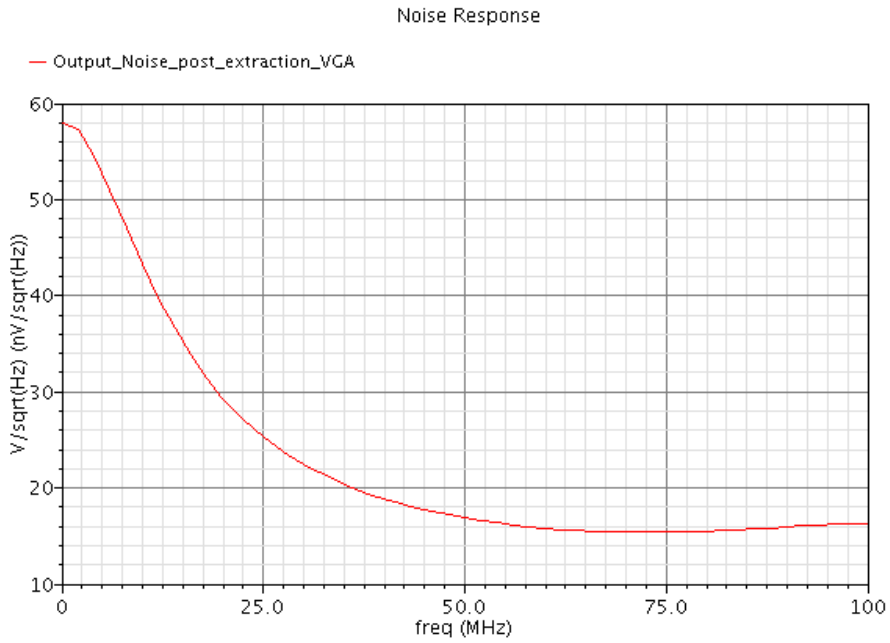


Figure 4-6 Noise simulation of wide dynamic range architecture

Table 4-3 Post extraction simulation results

| **Parameter** | **Post extraction simulation** |
|---|---|
| Output voltage | 0.13V-1.2V |
| Total integrated noise | 430.7µVrms (100MHz BW) |
| Power dissipation | 280.1µW |

*Measurement Results*

Figure 4-7 shows the die photograph of fabricated chip. Fabricated chip is then packaged and Figure 4-8 shows the photograph of packaged chip. In order to test the chip firstly a chip socket is soldered on to the adapter board as shown in Figure 4-9. Chip is then put in the socket. Sensor model is assembled on the bread board and connections are made from adapter board to bread board. Figure 4-10 shows the

measurement setup. Keithley 2400 source-meters are used to measure sensor current and output voltage. Agilent power supply is used to power on the chip. Measurement and simulation results are plotted together in Figure 4-11 for comparison purpose. It can be seen that measured and simulated results closely match.

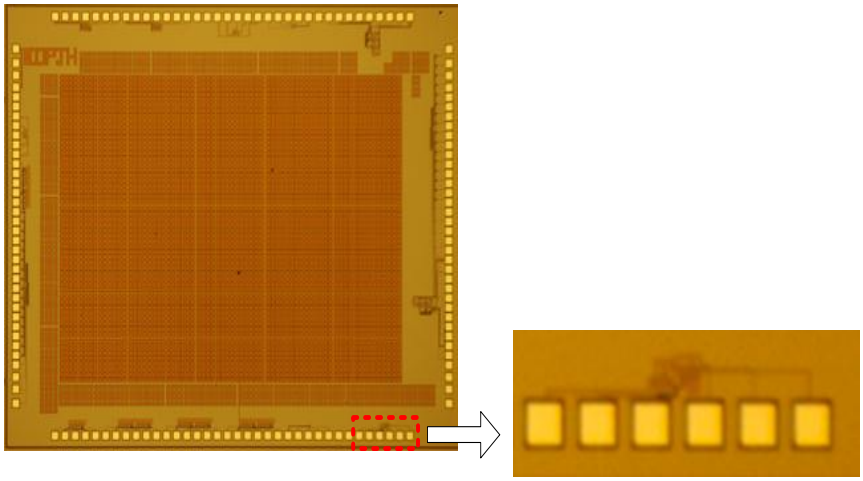

Figure 4-7 Die photograph of circuit


Figure 4-8 Packaged chip photograph

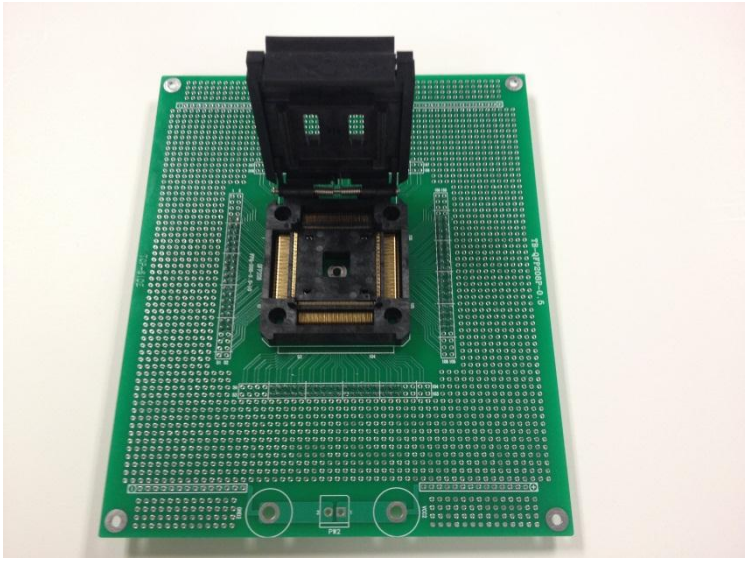

Figure 4-9 Chip socket with adapter board

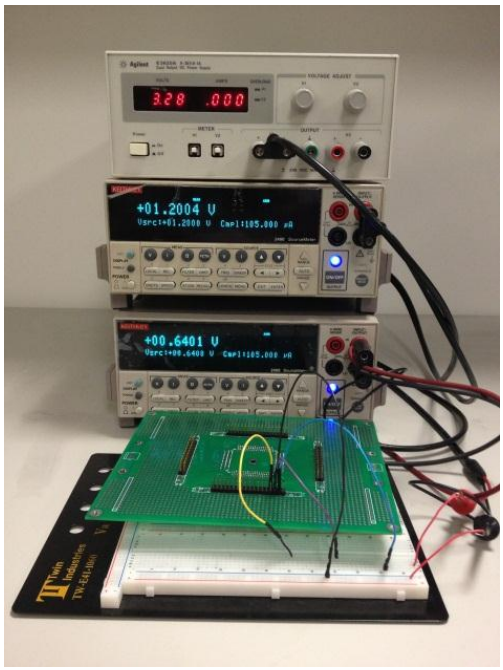


Figure 4-10 Measurement Setup

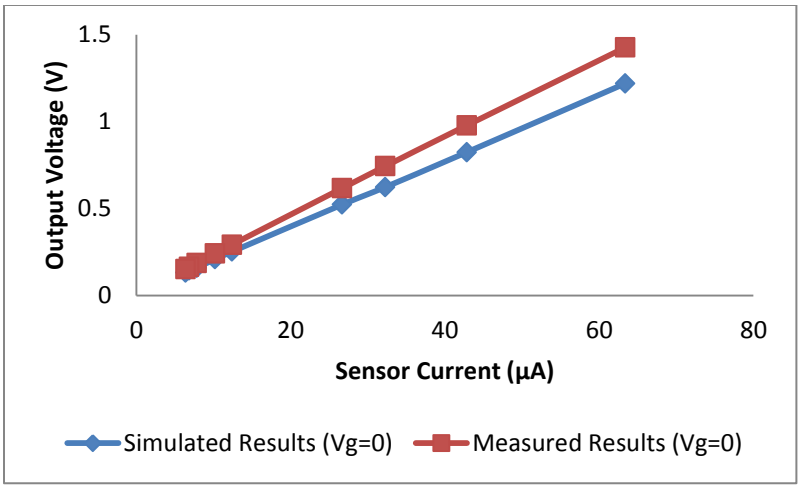


(a)

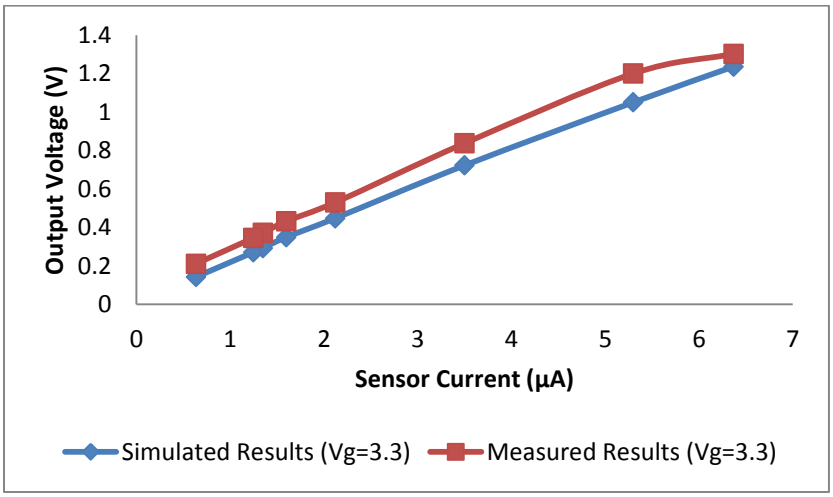


(b)

Figure 4-11 Measurement Results (a) When vg=0 (b) when Vg=3.3V

Maximum error between simulation and measurement results is 14%. Error occurs mainly because of chip parasitic and packaging parasitic. Also fabrication process induces certain mismatches between the components (for example in transistor lengths and width can vary, exact value of resistor can vary). Figure 4-12 shows the noise measurement results. Noise is measured with the help of oscilloscope. Since

oscilloscope measured the transient or time domain vales, RMS values are used to measure the noise. Total noise thus measured is around 444µVrms. Result closely matches with the simulation and suggests the minimum signal that can be detected by the system. Lower the noise higher the sensitivity of the system.

.

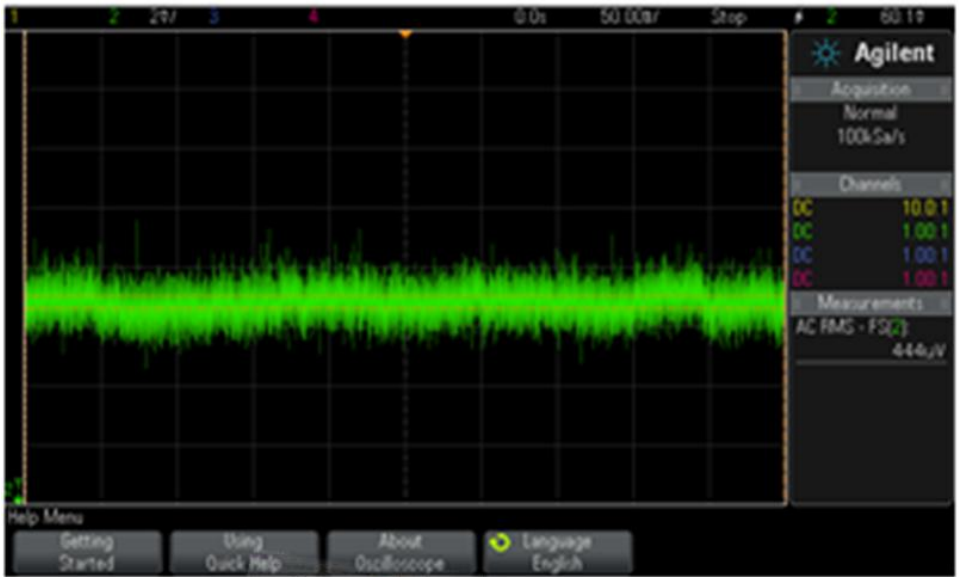


Figure 4-12 Noise Measurement

Table 4-4 shows the comparison between simulations and measurement results . It can be seen that measurement results closely match simulation results. Result also show that important performance criterions (like low power, low noise and compactness) for ultraportable glucose sensing applications like smart phone integration and implantable glucose sensing are met by this novel architecture. Also this architecture can used to sense low as well as high concentration of glucose by varying the gain of the circuit.

Table 4-4 Comparison between measurement and simulation results

| Parameter | Post extraction simulation | Measurement |
|---|---|---|
| Output voltage | 0.13V-1.2V | 0.15V-1.3V |
| Total integrated noise | 430.7μVrms | 444μVrms |
| Power dissipation | 280.1μW | 217.6μW |

In order to validate the circuit, measurements are done with actual three electrode amperometric glucose sensor. Figure 4-13 shows the measurement setup. The package chip is put in the socket and pins are interfaced with glucose sensor. For measurements four different concentrations of glucose solution are prepared (1, 1.5, 2, 2.5, 5, 8,10mM) so as to cover the all the three conditions namely Hypoglycemia (low blood glucose level below 4mM), Euglycemia (normal blood glucose levels 4-7mM) and hyperglycemia (high blood glucose levels above 7mM) along with range for glucose levels in tear fluid.. In order to make glucose solution 180.16gms of glucose (molecular weight of glucose) is weighed and then mixed into one liter of PBS (phosphate buffer saline) solution. This gives solution of 1M. This solution can then be diluted to make the different concentrations of glucose solution. Three electrode glucose sensors is immersed in the glucose solution and connection are made with the chip. Figure 4-14 shows the measured results. Results show that when control voltage is zero volts glucose levels measured are from 2.5mM to 10mM while when control voltage is 3.3V glucose levels measured are from 1-2mM.

Results show linear relationship between glucose concentration and output voltage. Thus circuit the variable gain architecture can be used to measure both blood glucose levels and glucose levels from tear fluid. Results show the same trend as

compared to the results with sensor model. Linearity shows that different glucose concentrations can be detected uniquely.

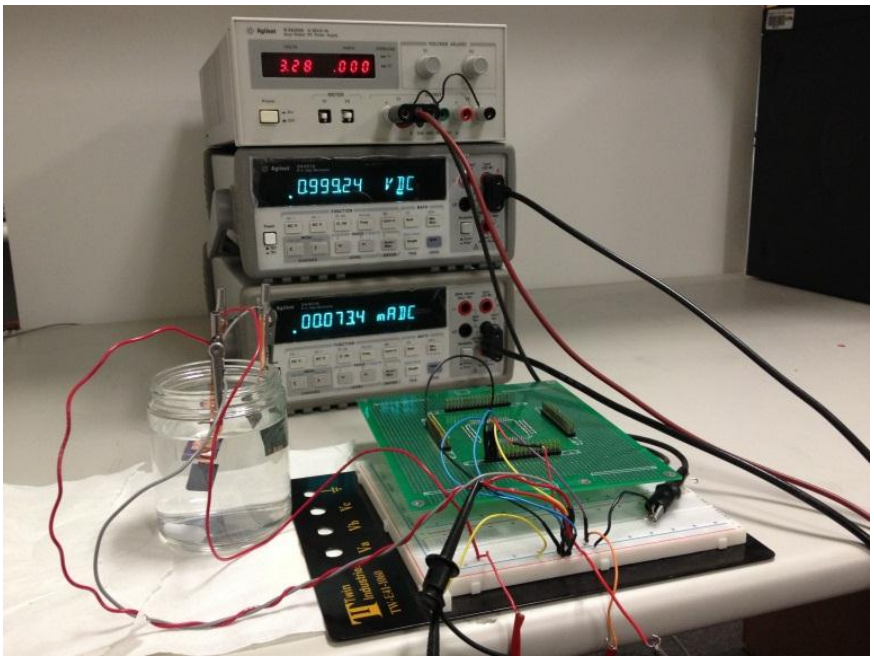

Figure 4-13 Measurement Setup

Table 4-5 Comparison of variable gain architecture with others

| **Architecture** | **Power consumption** | **Noise** | **Complexity** |
|---|---|---|---|
| Trans-impedance[30] | ≈4.3mW | N/A | Less |
| Trans-impedance variant[29] | 8.64mW | N/A | More |
| Switched capacitor[10] | 1.1mW | ≈2mVrms | Very complex |
| This work | 217.6µW | 444µVrms | Compact |

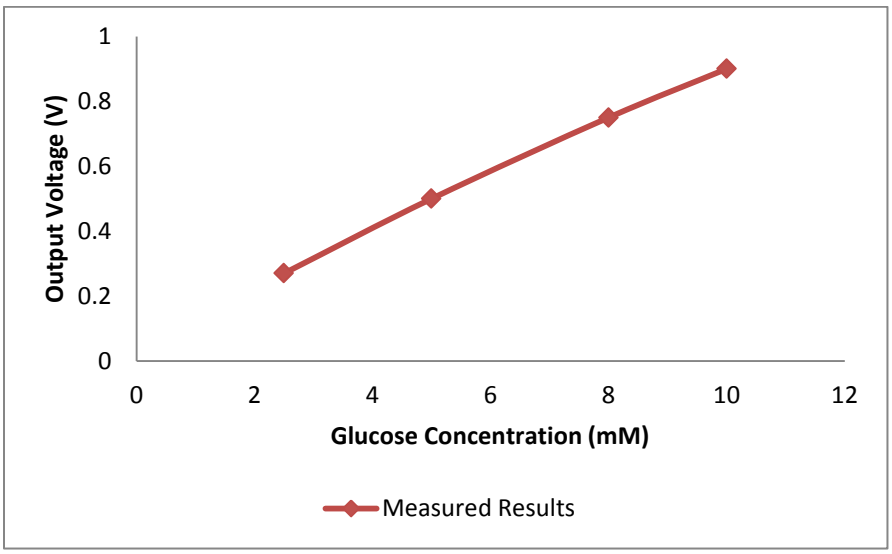


(a)

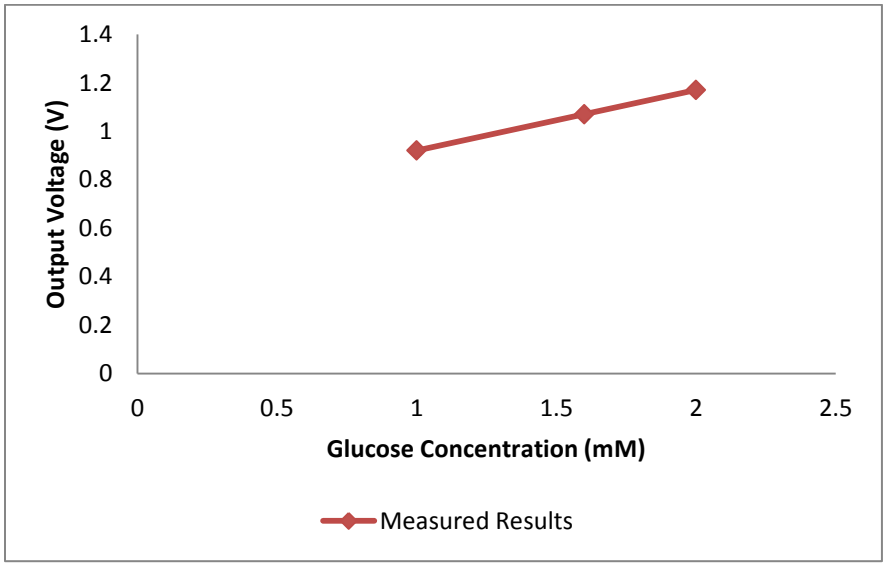


(b)

Figure 4-14 Measured Output Voltage Vs glucose concentration when (a) control voltage is zero (b) control voltage is 3.3V

Table 4-5 shows the comparison of this work with previous architectures. Power consumed by proposed variable gain architecture is 217.6μW which very small compared to the other architectures. This means that proposed architecture can give greater battery life needed for ultraportable applications. Also noise generated is 444μVrms which means small signals can be detected. It is also shown that output voltage is varies linearly with the glucose concentration.

Thus proposed architecture is more compact, generates less noise and consumes much less power. This architecture is suited for the ultra-portable glucose sensing applications like smart phone integration and implantable glucose sensing. Also ability to vary the gain of the circuit makes it suitable to measure high as well as low concentration of glucose.

# Chapter 5

## Conclusion

Diabetes is disorder associated with an insufficiency of insulin secretion. Constant monitoring glucose levels are very important for diabetic people. Several commercially available glucose meters are available for this purpose. Glucose meter has two parts; one is the referred to as a test strip and another as an interfacing circuit. Test-strip is a small electrochemical cell which converts glucose concentration into proportional current. Interfacing circuit has two components- a potentiostat maintains a constant potential between reference and a working electrode which is required for reaction. Reaction current is then read by current readout circuit which converts reaction current into voltage.

Handheld glucose meters are only one of the methods to monitor the glucose levels. Now a days there is a lot of research to use smart-phone as a glucose meter. Implantable glucose sensors which can monitor glucose levels in real time are also a subject of great research. These new applications require new circuit architectures to meet the specifications forced by them.

Even though monitoring blood glucose levels is one of the most common methods to detect the diabetes, other biological fluids like tear fluid can also be used to detect levels of glucose. With emergence of MEMS technology several biosensors are being developed, less invasive or non-invasive, which can detect these glucose levels from blood or tear. Central idea behind the developments of these biosensors is to have a glucose monitoring system which is portable and/or implantable. Biosensors developed for these applications thus requires an electronic interface, to readout biosensor output, which is compact, less power hungry and noisy. In this work power efficient, and less noisy electronic interface which can either be used to detect glucose levels from tear fluid

(1-2mM glucose concentration) or from blood (2.5-10mM glucose concentration) is developed.

In this work two novel architectures for glucose sensing are presented. First architecture can be used to detect glucose levels from blood while second architecture, called variable gain architecture, can be used to detect glucose levels from blood samples and from tear fluid.

Existing architectures requires two separate circuit one to control reaction potential while other to readout reaction current. All of the architectures are based on opamp and do not fully appreciate the power of integrated circuits. These architectures are power hungry and noisy. Architectures presented in this work have following salient features

- Threshold voltage is used as a reference voltage there by eliminating the need to generate the reference voltage
- Current is routed to output my current mirror configuration
- Architecture effectively integrates the functions of potentiostat and current readout circuit
- No operational amplifiers are required there by making circuit very compact, in other words architecture fully appreciates the power of integrated circuit and presents a customized solution than a general one
- In idle state power is consumed by bias current of four transistor which is very small
- Output noise is contributed by only three transistors thus making it low noise solution
- Working electrode is connected to actual ground there by eliminating environmental noise pickup

Architecture presented for glucose sensing from blood consumes 199µW of power while generating 312µVrms noise. Architecture can be used to detect the glucose levels from 2.5mM-10mM. Circuit occupies 125µm*340µm area.

Table 5-1 Architecture comparison

| **Architecture** | **Power consumption** | **Noise** | **Complexity** |
|---|---|---|---|
| Trans-impedance[30] | ≈4.3mW | N/A | Less |
| Trans-impedance variant[29] | 8.64mW | N/A | More |
| Switched capacitor[10] | 1.1mW | ≈2mVrms | Very complex |
| Low power, low power potentiostat architecture (This work) | 199µW | 312µVrms | Compact |
| Wide dynamic range architecture | 217.6µW | 444µVrms | Compact |

Wide dynamic range, variable gain architecture presented in this work can be used to detect glucose concentration from blood (high glucose concentration) and also from tear fluid (low glucose concentration). Circuit consumes 217.6µW of power while generating 444µVrms noise. Architecture can be used to detect the glucose levels from 1mM-10mM. Circuit occupies 116µm*551µm area.

Table 5-1 shows the comparison of architectures presented in this work with others. It can be seen architecture presented in this work consumes low power and generates very low noise. Architectures are also very compact and shown to detect glucose levels from 1mM to 10mM. Thus these architectures can be used for ultraportable application like smart phone integration and implantable glucose sensing.

References

[1] “How Our Bodies Turn Food Into Energy.” [Online]. Available: http://www.ghc.org/healthAndWellness/?item=/common/healthAndWellness/conditions/diabetes/foodProcess.html. [Accessed: 26-Sep-2013].

[2] D. D. Cunningham and J. A. Stenken, Eds., “In Vivo Glucose Sensing,” in *In Vivo Glucose Sensing*, John Wiley & Sons, Inc., 2009, pp. 445–450.

[3] Y.-T. Liao, H. Yao, A. Lingley, B. Parviz, and B. P. Otis, “A 3- CMOS Glucose Sensor for Wireless Contact-Lens Tear Glucose Monitoring,” *IEEE J. Solid-State Circuits*, vol. 47, no. 1, pp. 335–344, 2012.

[4] J. D. Lane, D. M. Krumholz, R. A. Sack, and C. Morris, “Tear glucose dynamics in diabetes mellitus,” *Curr. Eye Res.*, vol. 31, no. 11, pp. 895–901, Nov. 2006.

[5] J. Baca and R. Myllylä, “Tear Fluid Photonic Crystal Contact Lens Noninvasive Glucose Sensors,” in *Handbook of Optical Sensing of Glucose in Biological Fluids and Tissues*, vol. 20082359, V. Tuchin, Ed. Taylor & Francis, 2008, pp. 387–417.

[6] J. E. Shaw, R. A. Sicree, and P. Z. Zimmet, “Global estimates of the prevalence of diabetes for 2010 and 2030,” *Diabetes Res. Clin. Pract.*, vol. 87, no. 1, pp. 4–14, Jan. 2010.

[7] E. Wilkins and P. Atanasov, “Glucose monitoring: state of the art and future possibilities,” *Med. Eng. Phys.*, vol. 18, no. 4, pp. 273–288, Jun. 1996.

[8] M. M. Ahmadi and G. A. Jullien, “Current-Mirror-Based Potentiostats for Three-Electrode Amperometric Electrochemical Sensors,” *IEEE Trans. Circuits Syst. Regul. Pap.*, vol. 56, no. 7, pp. 1339–1348, 2009.

[9] R. Greef, “Instruments for use in electrode process research,” *J. Phys. [E]*, vol. 11, no. 1, p. 1, Jan. 1978.

[10] J. Zhang, N. Trombly, and A. Mason, “A low noise readout circuit for integrated electrochemical biosensor arrays,” in *Proceedings of IEEE Sensors, 2004*, 2004, pp. 36–39 vol.1.

[11] R. Doelling, “Potentiostats,” Application Note,2nd edition, Mar. 2000.

[12] “Electrochemistry Encyclopedia -- What is electrochemistry?” [Online]. Available: http://electrochem.cwru.edu/encycl/art-i02-introduction.htm. [Accessed: 22-Aug-2013].

[13] A. J. Bard and L. R. Faulkner, *Electrochemical methods: fundamentals and applications*. New York: Wiley, 2001.

[14] Miroslav Pohanka and Petr Skladal, “Electrochemical biosensors – principles and applications,” *J. Appl. Biomed.*, vol. 6, no. 2, pp. 57–64, 2008.

[15] J. Chou, *Hazardous gas monitors: a practical guide to selection, operation and applications*. New York: McGraw-Hill, 2000.

[16] J. Janata, “Electrochemistry Encyclopedia -- Electrochemical sensors.” [Online]. Available: http://electrochem.cwru.edu/encycl/art-s02-sensor.htm. [Accessed: 10-Sep-2013].

[17] M. M. Ahmadi and G. A. Jullien, “A wireless-implantable microsystem for continuous blood glucose monitoring,” *IEEE Trans. Biomed. Circuits Syst.*, vol. 3, no. 3, pp. 169–180, Jun. 2009.

[18] B. R. Eggins, Ed., “Introduction,” in *Analytical Techniques in the Sciences*, John Wiley & Sons, Ltd., 2007, pp. 1–9.

[19] V. Shenoy, “CMOS analog correlator based glucose sensor readout circuit,” Ph.D., The University of Texas at Arlington, United States -- Texas, 2013.

[20] M. M. Ahmadi, “A wireless implantable microsystem for continuous blood glucose monitoring,” Ph.D., University of Calgary (Canada), Canada, 2007.

[21] J. Wang, “Electrochemical glucose biosensors,” *Chem. Rev.*, vol. 108, no. 2, pp. 814–825, Feb. 2008.

[22] W. Zhang and G. Li, “Third-generation biosensors based on the direct electron transfer of proteins,” *Anal. Sci. Int. J. Jpn. Soc. Anal. Chem.*, vol. 20, no. 4, pp. 603–609, Apr. 2004.

[23] S. Park, H. Boo, and T. D. Chung, “Electrochemical non-enzymatic glucose sensors,” *Anal. Chim. Acta*, vol. 556, no. 1, pp. 46–57, Jan. 2006.

[24] T. R. G. C. Kathryn E, “Electrochemical Non-enzymatic Glucose Sensors: A Perspective and an Evaluation,” *Int J Electrochem Sci Int. J.*, vol. 5, pp. 1246–1301, 2010.

[25] M. S. Boyne, D. M. Silver, J. Kaplan, and C. D. Saudek, “Timing of changes in interstitial and venous blood glucose measured with a continuous subcutaneous glucose sensor,” *Diabetes*, vol. 52, no. 11, pp. 2790–2794, Nov. 2003.

[26] D. Pletcher, “Electrocatalysis: present and future,” *J. Appl. Electrochem.*, vol. 14, no. 4, pp. 403–415, Jul. 1984.

[27] S.-M. Park and J.-S. Yoo, “Electrochemical Impedance Spectroscopy for Better Electrochemical Measurements,” *Anal. Chem.*, vol. 75, no. 21, p. 455A–461A, 2003.

[28] L. Busoni, M. Carlà, and L. Lanzi, “A comparison between potentiostatic circuits with grounded work or auxiliary electrode,” *Rev. Sci. Instrum.*, vol. 73, no. 4, pp. 1921–1923, Apr. 2002.

[29] S. M. Martin, F. H. Gebara, T. D. Strong, and R. B. Brown, “A Fully Differential Potentiostat,” *IEEE Sensors J.*, vol. 9, no. 2, pp. 135–142, 2009.

[30] “LTC2050 Data sheet.” .

[31] P. R. Gray, *Analysis and design of analog integrated circuits*. New York: Wiley, 2009.

[32] B. Razavi, *Design of analog CMOS integrated circuits*. Boston, MA: McGraw-Hill, 2001.

[33] Y. Yoon, J. Kim, K. Lee, H. Song, K. Yoo, G. Lee, and J. Lee, “A novel microneedle-based non- enzymatic glucose sensor for painless diabetes testing application,” in *Solid-State Sensors, Actuators and Microsystems Conference (TRANSDUCERS), 2011 16th International*, 2011, pp. 2164–2167.

[34] G. S. Wilson and Y. Zhang, “Introduction to the Glucose Sensing Problem,” in *In Vivo Glucose Sensing*, D. D. Cunningham and J. A. Stenken, Eds. John Wiley & Sons, Inc., 2009, pp. 1–27.

## Biographical Information

Niranjan Karandikar is a candidate for Ph.D. in Electrical Engineering at University of Texas at Arlington. Niranjan completed his Bachelor's degree in Electronics Engineering from University of Mumbai in summer 2006. He then joined University of Texas at Arlington and received his M.S. in Electrical Engineering in summer 2008.

He started working on his Ph.D. under the supervision of Dr. Sugnyong Jung from fall 2008. He worked on several research projects like CMOS analog correlator design for for automotive radars, THz signal generation, high isolation mixer design, and readout circuits for biomedical applications during his Ph.D. Niranjan has research interest in high frequency, low power circuit design. He currently works at Intel Corporation, Santa Clara as RF Engineer.

.